Total Controllability Analysis Discovers Explainable Drugs for Covid-19 Therapy and Prevention

Xinru Wei[1,2,+], **Chunyu Pan**[3,+], **Xizhe Zhang**[1,2,*], **Weixiong Zhang**[4,5,*]

1. Early Intervention Unit, Department of Psychiatry, The Affiliated Brain Hospital of Nanjing Medical University, Nanjing, Jiangsu 210029, China;

2. School of Biomedical Engineering and Informatics, Nanjing Medical University, Nanjing, Jiangsu 210001, China

3. School of Computer Science and Engineering, Northeastern University, Shenyang, China

4. Department of Computer Science and Engineering, Department of Genetics, Washington University in St. Louis, St. Louis, MO, USA

5. Department of Health Technology and Informatics, The Hong Kong Polytechnic University, Hong Kong, China

+: Equal contribution.

*: Correspondence: WZ: weixiong.zhang@polyu.edu.hk; XZ: zhangxizhe@njmu.edu.cn

ABSTRACT

Network medicine has been actively pursued lately for repurposing drugs for Covid-19. One such approach adopts structural controllability, a theory developed for controlling a network (the cell). Motivated to protect the cell from viral infections, we extended this theory to total controllability and introduced a new concept of control hubs. Perturbation to any control hub renders the cell uncontrollable by exogenous stimuli such as viral infections, so control hubs are ideal drug targets. We developed an efficient algorithm for finding all control hubs and applied it to the largest homogenous human protein-protein interaction network. The novel control-hub-based method is superior to several popular gene-finding approaches for drug repurposing, including that based on structural controllability. The final 65 druggable control hubs are enriched with functions of cell proliferation, cellular response to stress, regulation of apoptotic signaling, and response to nutrient levels, revealing critical pathways induced by SARS-CoV-2. These druggable control hubs gave rise to drugs in four major categories: antiviral and anti-inflammatory agents, drugs on central nerve systems, and dietary supplements and hormones that help boost immunity. The functions and biological processes that the druggable control hubs involved with not only revealed the diverse cellular responses during SARS-CoV-2 infection but provided deep insight into the therapeutic mechanisms of the drugs for Covid-19 therapy, making the new approach an explainable drug repurposing method. A remarkable example is Fostamatinib, a medicine that was originally approved for chronic immune thrombocytopenia but was shown in a preclinical trial to lower mortality, shorten the length of ICU stay, and reduce disease severity of hospitalized Covid-19 patients. Fostamatinib targets 10 control hubs, 9 of which are kinases that play key roles in cell proliferation, differentiation, and programmed death. Among the 9 kinases is serine/threonine kinase RIPK1 which directly interacts with viral nonstructural protein nsp12, the RNA-dependent RNA polymerase of SARS-CoV-2. The current study also produced a set of control hubs that were not targets of existing drugs, which were enriched with membrane proteins and proteins on the NF-κB signaling pathway, so are excellent candidate targets for new drugs.

Introduction

The devastating Covid-19 pandemic caused by the severe acute respiratory syndrome coronavirus 2 (SARS-CoV-2)[1-4] has wreaked global havoc on all walks of life. SARS-CoV-2 and its variants have so far infected more than 515 million people and claimed more than 6 million lives worldwide as reported to WHO (https://covid19.who.int; as of April 2022). The numbers are climbing despite several vaccines have been administrated in many countries. The viruses, particularly the latest omicron variants[5], can penetrate the protection of the vaccines and spread rapidly in densely populated areas. Therefore, it is urgent to develop effective drugs for the treatment of SARS-CoV-2 infection.

Drug discovery is notoriously costly and time-consuming[6] and the development of new drugs for Covid-19 is challenging[7,8]. To shorten the period of drug discovery, one effective approach is to reposition or repurpose the drugs that were originally developed for other diseases, a major focus of the latest pursuit of effective drugs for Covid-19[9-14]. However, the space for drug repurposing is enormous[11,15] and depending on the overall approach taken, consists of clinical studies[14,16], screening of molecular structures and dynamics of protein-ligand binding[17], and computational analysis of the properties of and relationships among genes, proteins, pathways, and diseases[13,18,19]. The most eminent computational approaches adopt the perspective of systems biology or network medicine[20-27]. Among these are methods based on the well-established structural controllability[24,25,28]. Following the theory of structural controllability[29-31], the cell is regarded as a network of genes/proteins that can be controlled by exogenous stimuli (e.g., viral infections or medical interventions) on a set of driver nodes (i.e., proteins) so that the cell can be driven from any state to the designated state in finite time. Structural controllability has been applied to protein-protein interaction networks[32], gene regulatory networks[33,34], and metabolic networks[35]. The concept of driver nodes matches with that of cancer driver genes[36] and thus has been applied to find cancer driver genes as therapeutic targets for precision cancer treatment[25,37].

While theoretically sound, it is impractical to directly apply structural controllability to drug repurposing. The key to the structural controllability of a network is a control scheme consisting of a set of control paths and their starting nodes (driver nodes or genes) that can be used to steer the network from any arbitrary state to the designated state in a finite time. Under this theory, a drug is used as an exogenous force to change the states of the cell, hopefully, from an infectious or cancerous state to a normal state. However, the normal states of a cell are typically unknown so it remains unclear what external stimuli or drugs should be used. Moreover, the control scheme is not unique, and a control scheme typically has too many driver nodes to be practically manipulated at once to control the cell.

We pushed the envelope of the theory of structural controllability. Not attempting to control the cell using external forces, we instead aimed at protecting the cell from any external influences such as viral infections. To this end, we expanded our perspective from structural controllability based on a single control scheme of a network to a global view of total controllability over all control schemes for the network. We then introduced the concept of control hubs, which are nodes residing on a control path of every control scheme of the network. The control hubs are the most vulnerable spots to the structural controllability of the network; a perturbation to any control hub may render the network uncontrollable by any control scheme. Therefore, control hubs are ideal drug targets for protecting the cell from exogenous influences like viral infections. Moreover, exploiting control hubs as drug targets is a more practical approach for drug repurposing because control hubs are typically an order less than driver nodes. Without computing all control schemes, which is a #P-hard problem[38] (meaning no polynomial-time or efficient algorithm is known), we developed a polynomial-time (meaning efficient) algorithm for finding all control hubs for a network. We applied our novel control hub-based, data-driven drug repurposing approach to the largest homogenous network of human protein-protein interactions[39] (PPIs, Supplemental Table S1), along with the data of PPIs between SARS-CoV-2 and human[40,41] (Table S2) and the data of drug targets[42] (Table S3), to discover a set of clinically available drugs that are potentially effective for treating SARS-CoV-2 infections.

Results

Extending structural controllability to an effective approach for drug repurposing

The primary concept of network structural controllability[29-31] is a control scheme for a network. A control scheme consists of control paths such that every node in the network can be reached or controlled by the head node of the control path to which the node belongs (Figure 1A). The head node is also referred to as the driver node or input node of the path. By applying external stimuli to the driver nodes of the scheme, the network can be controlled, i.e., the network can be steered from any initial state to the designated state in a finite time.

Viral infections to the cell are a type of exogenous stimuli through the interactions of viral proteins and host receptors, which can drive the latter out of its normal states to some abnormal states for viral replication and propagation. In the case of SARS-CoV-2 infection, the viral spike protein S[43] engages human receptor angiotensin-converting enzyme 2 (ACE2) to enter the host cell and consequentially trigger a series of adverse signaling cascades[44]. Conversely, drug therapy blocks some of the viral-host interactions[45] to prevent infection or to intervene in some interactions among the host proteins to prohibit viral propagation.

Notably, the control scheme is not unique (Figure 1A), there may exist an exponential number of control schemes, and determining the best or an effective control scheme is a daunting task. Moreover, numerous driver nodes exist as well, as many as half of the nodes in the network for even one control scheme. For example, the human PPI network[39] (see Methods) has 4,529 driver nodes for one control scheme, which is 49.8% of the 9,092 nodes in the network (Table S1). Therefore, it is neither effective nor practical to directly apply structural controllability to look for effective drugs for Covid-19.

We were interested in critical nodes of a network that, when perturbed, can render the network uncontrollable for any control scheme of the network. Manipulation of any of such critical nodes can invalidate all the control schemes, so the network is uncontrollable by undesired stimuli. To identify such critical nodes, we extend structural controllability to *total controllability* by considering all control schemes altogether and introducing a novel concept of control hubs (see Methods). A *control hub* is a middle node in one of the control paths of every control scheme (Figure 1B). Blocking a control hub will block at least one control path of every control scheme, making the overall network uncontrollable.

The motivation and rationale for introducing control hubs are completely different from that for driver nodes. Control hubs are used to protect the cell from external stimuli, whereas driver nodes are defined to control, drive, or perturb the cell to force it to make state transitions. Therefore, control hubs are ideal drug targets for protecting the cell being manipulated by viral infections. If the nodes that viruses act on are known, the control hubs close to these nodes can be chosen as designated drug targets to increase drug efficacy. In contrast, following the structural controllability theory, a drug targeting a driver gene is supposed to drive the cell from an infected state to a normal state, which is a difficult task to accomplish.

Since the concept of control hubs is built atop all control schemes, one technical obstacle is the large, potentially exponential number of valid control schemes for a network. Finding all control schemes using the current best method, i.e., maximum matching[46], is a #P-complete problem[38], i.e., no polynomial-time algorithm is currently known for the problem. To circumvent this difficulty, we developed a polynomial-time (meaning efficient) algorithm for identifying all control hubs without computing all control schemes (see Methods). The algorithm identified 1,256 control hubs in the human PPI network[39], which are 13.8% of the 9,092 nodes in the network and 27.7% of the 4,529 driver nodes for the network (Table S1).

With the control hubs in hand, we can then use them as surrogates for drug repurposing, i.e., we focus on those existing drugs that can target control hubs. While in theory, any drug-targeted control hubs can be used, the ones that are closer to exogenous stimuli (i.e., viral proteins) are preferred over the distant ones since blocking the former may prevent the spread of external influences sooner and more effectively.

Control hubs as drug targets for the treatment of SARS-CoV-2 infection

We capitalized on the concepts of total controllability and control hubs to develop an effective, explainable approach for drug purposing (Figure 2A; see Methods). We focused on the control hubs that were known targets of the existing drugs, which were categorically referred to as *druggable control hubs* hereafter. Among the 1,256 control hubs in the human PPI network, 160 (12.7%) were drug targets (Figure 2B). We reasoned that not all druggable control hubs were equally effective to treat or prevent SARS-CoV-2 infection. Some may directly interact with viral proteins and thus are ideal drug targets, whereas many others are far away from viral proteins in the human PPI network (Figure 2A). The closer a druggable control hub to virus proteins in the network, the more effective it should be for prohibiting viral infection.

We examined the druggable control hubs in the community of proteins that were *k* steps away from the virus proteins in the PPI network, which was referred to as the *k*-step community for convenience. A smaller *k* is preferred; the closer a control hub is to viral proteins, the more effective it is as a drug target to block viral infections. Two sets of enrichment tests, using the z-test, were performed to identify the best *k*-step community (see Methods). The first set of tests looked for the *k*-step community that was most enriched with control hubs among all *k*-step communities for different values of *k*, and the second set of tests assessed the enrichment of drug targets among the control hubs in the community chosen by the first test. The first z-test across all possible *k* values revealed that the 2-step community was most enriched with control hubs (z-score=28.25, *p*-value=1.3e^{-175}, Figures 2C, S1A). It hosted 677 control hubs, among which 65 were drug targets (Table S4A). The second set of z-test confirmed that the 2-step community was also most enriched with druggable control hubs among all *k*-step communities (z-score=5.28, *p*-value=1.3e^{-7}, for *k*=2, Figures 2D, S1B).

To evaluate if our novel control-hub approach was indeed the method of choice for finding drug targets, we compared it with the driver-node method and eight popular gene selection and node ranking methods. These included node-degree centrality, neighbor-degree centrality, betweenness centrality, load centrality, closeness centrality, and eigenvector centrality, as well as page rank, and k-core[47-56] (see Methods). To facilitate the comparison and better understand these methods, we compared them against a statistical baseline model of drug targets in the 2-step community. Assuming that being a drug target was a random event for any protein in the 2-step community, the drug-target enrichment for 677 (i.e., the number of control hubs in the 2-step community) randomly selected proteins in the community should follow an empirical, normal distribution (Figure 2E; see Methods). This empirical distribution was adopted as the statistical baseline model of drug-target enrichment. The enrichment of the 65 drug targets among the 677 control hubs in the 2-step community substantially deviated from the baseline model (*z*-score=1.53, *p*-value=0.13; Figure 2E). Likewise, the drug-target enrichment for 677 driver nodes randomly chosen from the total of 965 driver nodes in the 2-step community should also obey an empirical, normal distribution (Figure 2E). The drug-target enrichment of the control-hub method was significantly better than that of the driver-node method (z-score=2.82, *p*-value=0.005). The driver-node method was slightly worse than the baseline model since the mean of the former was smaller than the mean of the latter (54.07 vs 56.05; Figure 2E) and the two distributions were statistically indistinguishable (*p*-value = 0.98, χ^2-test; Figure 2E). We measured the drug-target enrichments of the top 677 nodes from the eight gene-ranking methods. Unfortunately, these methods were all underperformed; their z-tests against the random baseline all resulted in negative z-scores (Figure 2E). For instance, the popular Page rank method had a z-score=-1.89 with *p*-value=0.06. In summary, this analysis showed that our control-hub method can help identify the largest numbers of drug targets and candidate drugs for Covid-19 treatment.

Among the 160 druggable control hubs, three (RIPK1, CYB5R3, and COMT) directly interact with nonstructural proteins of SARS-CoV-2[40,41] (Figures 2F, 2G, S2; Tables 1, S4A). Remarkably, RIPK1 can bind with viral nonstructural protein nsp12[40,41], the RNA-dependent RNA polymerase (RdRp) of SARS-CoV-2[57] (Figures 2F, 2G). nsp12 not only promotes viral replication but also inhibits the host's innate immune response by suppressing the activity of human interferon regulatory factor 3 (IRF3), which is key to interferon production[58]. Both CYB5R3 and COMT interact with the nsp7 protein of SARS-CoV-2 (Figures 2F, 2G), which forms a tetramer with viral nsp8[59] and functions as a cofactor of the viral RdRp, nsp12[57]. Since nsp12 and nsp7 are essential for viral

transcription and replication, blocking the interactions of RIPK1 with nsp12, CYB5R3 with nsp7, and COMT with nsp7 can potentially inhibit or suppress viral replication.

RIPK1 encodes serine/threonine-protein kinase 1, plays a role in necroptosis, apoptosis, and inflammatory response, and functions as a mediator of cell death and inflammation[60,61]. SARS-CoV-2 infection promotes the expression of RIPK1 in the lung of Covid-19 patients and small-molecule inhibitors of RIPK1 can reduce the viral load of SARS-CoV-2 and proinflammatory cytokines in human lung organoids, indicating that the virus hijacks RIPK1-mediated immune response for its replication and propagation[62]. RIPK1 is a target of Fostamatinib (Table 1, S4A; Figure 2F), a drug that has lately been under intense scrutiny for treating SARS-CoV-2 infection[63-68]. Fostamatinib is an inhibitor of spleen tyrosine kinase originally approved for treating chronic immune thrombocytopenia, a complication due to an abnormally low level of platelets. It is effective in a mouse model of acute lung injury and acute respiratory syndrome, symptoms observed in Covid-19 patients[64]. A clinical trial with a small sample of hospitalized Covid-19 patients (30 with fostamatinib versus 29 with placebo) showed that Fostamatinib can lower mortality, shorten the length of ICU stay, and reduce the disease severity of critically ill patients[65] (more discussion below).

CYB5R3 encodes NADH-cytochrome B5 reductase 3, a flavoprotein with oxidation functions. It is targeted by three drugs (Tables 1, S4A), two of which, NADH and Flavin adenine dinucleotide, are under clinical investigation for Covid-19 treatment. NADH is an energy booster for treating chronic fatigue syndrome and improving high blood pressure and jet lag, among many other symptoms. NADH, i.e., nicotinamide adenine dinucleotide (NAD)+ hydrogen (H), is the central catalyst of cellular metabolism, a chemical naturally produced in the human body and plays a role in ATP production. The SARS-CoV-2 genome does not encode enzymes for ATP generation and the virus needs to hijack host functions for viral synthesis and assembly. Therefore, NAD is regarded as a battlefield for viral infection and host immunity[69]. Indeed, coronavirus infection dysregulates the NAD metabolome, as indicated in a preclinical study[70]. Moreover, early phases 2 and 3 clinical trials showed that medication of NADH in a mixture of two metabolic activators can significantly shorten the time to complete recovery of SARS-CoV-2 infection[71].

COMT encodes catechol-O-methyltransferase that can degrade estrogens, catecholamines, and neurotransmitters such as dopamine, epinephrine, and norepinephrine. It is targeted by 15 drugs with 14 FDA-approved including Conjugated estrogens (Tables 1, S4A). Conjugated estrogens are a mixture of estrogen hormones for the treatment of hypoestrogenism-related symptoms. Estrogen has been indicated as a susceptibility factor of SARS-CoV-2 infection[72], as women are less susceptible to Covid-19[73,74] and mice with weaker estrogen receptor signaling due to respiratory coronavirus infection exhibit increased morbidity and mortality[75].

Beyond the 3 druggable control hubs that directly interact with viral proteins, 19 druggable control hubs in the 2-step community engage more than one viral protein via another protein, and four of them (SLC10A1, SLC10A6, MUC1, and TTPA) are targeted by more than one drug (Tables 1, S4A; Figure S2). SLC10A1 and SLC10A6 are members of the family of sodium/bile acid cotransporters, also known as Na^+-dependent taurocholate cotransporting polypeptides (NTCP). Besides the involvement in cholesterol homeostasis, SLC10A1, the founding member of the SLC10A family, takes part in HBV and HDV infections as a receptor of viral entry[76]. Such antiviral activities allude to its potential function in SARS-CoV-2 infection. SLC10A1 is targeted by 18 drugs, among which 9 have entered clinical trials for Covid-19 treatment, and SLC10A6 by two drugs. Four of these 18 drugs targeting SLC10A1 are worth mentioning. The first is Conjugated estrogens, which also target COMT, as discussed earlier. The second is Progesterone, another type of female hormone (Progestin), which can boost innate inflammatory responses. It is effective in reducing the severity of Covid-19 in pilot clinical studies[77,78]. The third is Indomethacin, a non-steroidal anti-inflammatory drug with functions of antitumor activities and antiviral activities against hepatitis B virus, rhabdovirus, and vesicular stomatitis virus. Importantly, it has been shown to relieve symptom severities and maintain oxygen saturation levels in Covid-19 patients[79,80]. The fourth is Cyclosporine A (CsA), an immunosuppressive drug widely used in the prevention of graft rejection in organ transplants. A few *in vitro* studies demonstrated the antiviral function of CsA against

SARS-CoV-2 replication[81-83], and several clinical trials are currently underway[84]. Interestingly, SLC10A6 is targeted by two drugs that are distinct from the ones targeting SLC10A1. The first drug, Pregnenolone, is a hormone naturally produced in the human adrenal gland or from cholesterol and is a precursor to many other hormones including Progesterone, Estrogen, and dehydroepiandrosterone (DHEA)[85]. While Pregnenolone has been often used in treating neuropsychiatric disorders, its potential function in Covid-19 is due to its emerging anti-inflammatory role in repressing the Toll-Like Receptor 4 (TLR4) signaling pathway[86] which plays an important part in initiating the innate immune response[87]. The second drug targeting SLC10A6 is Prasterone sulfate or dehydroepiandrosterone sulfate (DHEA-S), which is a natural androstane steroid released from the adrenal gland and used as a labor inducer in childbirth. DHEA-S has been indicted in inflammatory diseases[85] and extremely low levels of DHEA-S have been detected in patients with septic shock due to cytokine storms[88]. Remarkably, DHEA-S and DHEA levels are inversely correlated with the abundance of serum interleukin-6 (IL-6)[89], whereas Covid-19 patients have a significantly elevated amount of proinflammatory cytokines, especially IL-6[3,4]. In short, the large number of drugs targeting the two members of the NTCP family attempt to boost essential hormones to enhance immunity against SARS-CoV-2 infection and suppress excessive proinflammatory cytokines that may potentially adversely cause organ damage.

MUC1 encodes a transmembrane protein in the mucin family that plays an essential role in forming protective mucous barriers on mucosal epithelial cell surfaces in various tissues and organs, including the lung, stomach, and pancreas[90]. An elevated abundance of MUC1 is indicative of the development of acute lung injury (ALI) and acute respiratory distress syndrome (ARDS)[91], which are symptoms of Covid-19 patients[92,93]. MUC1 is targeted by Potassium nitrate, an ingredient in toothpaste to alleviate tooth sensitivity to temperature and acids. A small clinical trial with 5 patients showed that the medicine helps bring the levels of oxygen saturation to above baselines in Covid-19 patients[94]. While MUC1 does not seem to be a direct target of Fostamatinib, which targets ten control hubs including RIPK1 (Tables 2, S5), it has been shown that Fostamatinib can reduce MUC1 expression as a repurposed drug for Covid-19[64].

TTPA is a protein that binds α-tocopherol, a form of vitamin E, and regulates vitamin E levels by transporting vitamin E between membrane vesicles and facilitating vitamin E secretion from hepatocytes to circulating lipoproteins. Clinical studies reveal that the baseline plasma levels of α-tocopherol are lower than the normal in patients with ARDS[95] and vitamin E is beneficial for relieving the burden of upper respiratory tract infections[96]. Therefore, it is not unexpected that TTPA is the target of six vitamin E supplements, which have been recommended as adjuvant therapy against SARS-CoV-2 infection[97,98].

Categorically, the 65 druggable control hubs within the 2-step community were enriched with biological functions related to cell (particularly leukocyte) proliferation, cellular response to (chemical) stress, regulation of apoptotic signaling, and response to nutrient levels (Figure 3A). All these results combined revealed the essential roles that these control hubs may play in preventing the replication and proliferation of SARS-CoV-2. The results also helped reveal the essential immune-related signaling pathways that were induced by the virus and paved the way for understanding and explaining the therapeutic mechanisms of the drugs for Covid-19 treatment.

Finally, the 2-step community also hosted 612 control hubs that were not targets of the existing drugs (Table S4B). We postulated that they were ideal candidate targets for new drugs. It was encouraging that these control hubs were enriched with membrane proteins and proteins functioning on the NF-κB signaling pathway (Figure S3), so the result invited further investigation for new drug discovery.

Effective drugs for the treatment of SARS-CoV-2 infection

The 65 druggable control hubs within the 2-step community were targeted by 185 existing drugs (Tables 2, S5; Figure 3B). Among these drugs, 38 are currently under clinical trial (https://clinicaltrials.gov/ct2/home). It is desirable to use drugs that have multiple targets to gain treatment efficacy; the potency of a drug can be estimated by the number of control hubs that it targets. Remarkably, 15 drugs target more than one control hub and 7 drugs target more than 2 druggable control hubs (Tables 2, S5).

Among the 7 drugs targeting more than 2 control hubs were Fostamatinib, NADH, and three calcium dietary supplements (Tables 2, S5). Fostamatinib is currently in phase 3 clinical trial after a promising phase 2 trial for Covid-19 treatment[65]. Experimental and clinical data showed that Fostamatinib inhibits neutrophil extracellular traps (NETs), which entrap and eliminate pathogens during viral and bacterial infections and may cause adversely injury to surrounding tissues by themselves or by increasing pro-inflammatory responses[99] (Figure 3C). Activation and overreaction of innate and adaptive inflammatory responses during SARS-Cov-2 infection induce NETs which contribute to immunothrombosis in ARDS commonly seen in Covid-19 patients[63,100-102]. Moreover, coherent anti-viral therapeutic functions of Fostamatinib emerged after examining the functions of the control hubs that the drug targets (Figures 3B, 3C; Table S5). Among the 10 control hubs that Fostamatinib targets, 7 (RIPK1, CLK2, CLK3, PAK5, STK3, PKN1, and CDK4) are serine/threonine type protein kinases and two (BLK and YES1) encode Src family tyrosine kinases, all of which play essential roles in cell proliferation, cell differentiation, and programmed cell death[103]. CLK2 and CLK3 encode members of the serine/threonine type protein kinase family, and PAK5, STK3, PKN1, and CDK4 encode, respectively, one of the three members of group II PAK family of serine/threonine kinases, serine/threonine-protein kinase 3, serine/threonine protein kinase N, and cyclin-dependent serine/threonine kinase. Plus, RIPK1 encodes receptor-interacting serine/threonine-protein kinase 1 and directly interacts with the viral RdRp nsp12 as discussed earlier. Interestingly, while not being a kinase, the remaining target COQ8A encodes a mitochondrial protein functioning in an electron-transferring membrane protein complex in the respiratory chain. Its expression is induced by the tumor suppressor p53 in response to DNA damage, and inhibition of its expression suppresses p53-induced apoptosis. Combined, the inhibitory function on NETs and kinase functions of 9 of the 10 control hubs targeted by Fostamatinib suggested it to be potent for Covid-19 treatment by acting broadly on components of autoimmune, tumor repression, and inflammatory viral response pathways (Figure 3C).

NADH targets 5 control hubs, including CYB5R3 and NDUFB7. CYB5R3 encodes NADH-cytochrome B5 reductase 3, and NDUFB7 is a subunit of the multi-subunit NADH:ubiquinone oxidoreductase. NDUFB7 functions in the mitochondrial inner membrane and has NADH dehydrogenase and oxidoreductase activities. It has been reported that the NADH level was decreased in Covid-19 patients[69] and coronavirus infection dysregulates the NAD metabolome[70], so medication of NADH plays a role in attenuating the impact of virus infection.

The three calcium dietary supplements, Calcium Citrate, Calcium Phosphate, and Calcium phosphate dihydrate, target three control hubs, including S100A13 and PEF1 which are calcium-binding proteins. A low serum calcium level has been indicated by various clinical studies as a prognostic factor of the mortality, severity, and comorbidity of SARS-CoV-2 infection[104-106]. As a side note, six vitamin E-related drugs targeting control hub TTPA (Table S5), which encodes a soluble protein that is a form of vitamin E (Tables 1, S5), have entered clinical trials for Covid-19 treatment. Combined, these results indicated that calcium, vitamin E, and many other micronutrients should be adopted as adjuvant therapy against viral infection.

In summary, the repurposed drugs fall into four major categories (Table S5), 1) antiviral and anti-inflammatory agents that are subscribed for virus infection and cancer treatment, 2) dietary supplements including NADH and Calcium that boost human immunity, 3) hormones, including conjugated estrogens, and 4) drugs acting on central nerve systems. Combined, the medicines in the first three categories help boost immunity to overcome the adverse stress and influence of viral infections.

Effective drugs for prevention of SARS-CoV-2 infection

The analysis so far focused on the control hubs that can potentially block viral transcription and replication and their downstream functions of suppressing host immunity and anti-inflammatory response. We were also interested in control hubs and drugs that can inhibit the viral entry into or spread in the host cells to prevent infection in the first place. Therefore, we considered the druggable control hubs that interact directly or engage the viral S protein.

SARS-Cov-2 viruses bind to host receptors through their S-glycoproteins, which mediate membrane fusion and viral penetration[43-45]. Sixteen membrane proteins have been indicted as host receptors or cofactors, which

directly interact with the S protein for SARS-CoV-2's entry into host cells[107] (Table S6). Seven of the 16 host receptors and cofactors are in the homogenous human PPI network, but only ASGR1 is a druggable control hub. Whereas the other nine, including the main human receptor ACE2[44,45], are not in the network. Thus, we assembled a larger human interactome using data from multiple databases (see Methods). ACE2 was a druggable control hub in the larger PPI network. We focused on the two druggable control hubs, ACE2 and ASGR1, which interact directly with the viral S protein (Tables 3, S6).

ACE2 encodes a single-pass, transmembrane protease, known as a major host receptor for SARS-Cov-2 (Tables 3, S6). ACE2 has a significantly higher (10-20 times more) bind affinity with SARS-Cov-2 than with SARS-COV-1[44,108]. This partially explains the higher transmissibility of SARS-CoV-2, although it is weakly expressed on the surface of epithelial cells in the oral and nasal mucosa and nasopharynx[109,110]. ACE2 is targeted by 23 drugs, including Bromhexine, Hydroxychloroquine, Azithromycin, Hydroxocobalamin, Ascorbic acid, and Vitamin D (Table S6). Bromhexine is a potent TMPRSS2 inhibitor, which may block viral entry by reducing the activity of the S protein and intercepting the interaction between the S protein and ACE2. A preliminary clinical trial with 78 hospitalized patients shows that Bromhexine can significantly reduce ICU admission and mortality[111]. Bromhexine is also found to be effective in reducing the rate of symptomatic COVID-19 among 50 healthcare workers[112]. Hydroxychloroquine and Azithromycin are two common drugs for the treatment and prevention of COVID-19 whereas their effects on COVID-19 treatment and prevention remain to be further tested[113-115]. Moreover, Hydroxocobalamin, Ascorbic acid, and Vitamin D, as Vitamin dietary supplements, can be adopted as a preventive therapy against viral infection.

ASGR1 can function as an alternative receptor of ACE2 and directly mediates SARS-Cov-2's entry[116,117]. It is expressed mainly in hepatocytes. it is targeted by Von Willebrand factor, whereas no clinical data is available showing its function in preventing or treating COVID-19.

We also considered the druggable control hubs that were two steps away from the S protein in the PPI network, which we referred to as the 2-step-S community. Fifteen druggable control hubs (ASGR1, BNIP3, CALM2, CALM3, CYB5R3, GJB1, GPX8, HIBADH, IGFBP5, KCNIP3, KLRC1, NCALD, OPRM1, SLC10A1, and TMPRSS4) emerged out of the 44 control hubs in the 2-step-S community (Table S7). Eight druggable control hubs (BNIP3, CALM2, CALM3, GPX8, KCNIP3, KLRC1, NCALD, and TMPRSS4) are targeted by drugs that are under ongoing clinical trials for Covid-19 treatment.

Calcium dietary supplements target BNIP3, CALM2, CALM3, and NCALD (Tables 3, S7). It has been shown that COVID-19 patients have lower serum calcium levels than healthy individuals[118]. Thus, calcium dietary supplements may be adopted as safe and low-cost measures to help prevent viral infection. They may also help lower the risk of severe progression and prognosis of SARA-Cov-2 infection[118].

GPX8 encodes glutathione peroxidase 8 and is targeted by Glutathione, a potent antioxidant that plays a critical role in protecting cells from oxidative damage[119]. A clinical study showed that higher levels of Glutathione may enhance an individual's immunity against viral infections[120]. Glutathione therapy is effective in relieving dyspnea associated with SARS-CoV-2 infection[121].

KCNIP3 encodes potassium voltage-gated channel interacting protein 3 that functions as a calcium-regulated transcriptional repressor. It is targeted by Potassium and Magnesium. Low levels of magnesium and potassium are common characteristics of most COVID-19 patients[122,123]. Moderate intake of magnesium and potassium could strengthen immune function and prevent viral infection[124,125], which is a safe and inexpensive over-the-counter prevention or treatment.

KLRC1 encodes killer cell lectin-like receptor C1, which is a transmembrane protein preferentially expressed in natural killer cells. It is targeted by six drugs, including Infliximab which is a tumor necrosis factor (TNF-α) inhibitor and has been used to treat a variety of inflammatory conditions, such as rheumatoid arthritis. Clinical data have shown that Infliximab therapy could rapidly control pathological inflammation, preventing further clinical deterioration for patients with severe COVID-19[126]. Infliximab targeting KLRC1 could be a good candidate for the prevention and treatment of Covid-19.

Transmembrane serine protease 4 (TMPRSS4) is a member of the serine protease family, which has a domain architecture like TMPRSS2[127]. It has been shown that TMPRSS4 facilitates the activities of the S protein by inducing the cleavage of the S glycoproteins and promoting virus entry into host cells[128]. Phenylmethanesulfonyl fluoride (PMSF) is an irreversible inhibitor of serine proteinases and targets TMPRSS4. The drug may be an excellent candidate for preventing Covid-19.

In summary, blocking the interaction of host receptors and/or cofactors with the S protein could potentially prevent viral infection, and the control hubs that engage with the S protein are excellent drug targets for virus defense. We identified candidate drugs targeting these control hubs (Tables 3, S7). Most of these drugs are dietary supplements (including Glutathione, Vitamin D, Calcium, Potassium, and Magnesium) that strengthen the immune system to prevent viral infection. The other drugs, e.g., Bromohexin, may act as potent inhibitors of TMPRSS2, to exert antiviral effects. Bromohexin is also inexpensive, widely available, and has a low side-effect and thus could be used as a candidate drug for the prevention of SARS-Cov-2 infections.

Discussion

Drug repurposing based on systems biology or network medicine[20-25] has gained popularity and momentum lately since the Covid-19 pandemic[20-23,29,31,37]. These methods can rapidly produce high-quality putative drug targets as well as drugs that are supported by experimental/clinical data. Most of these network-biology methods, ours included, hinge upon the idea that important proteins can be used as surrogates for identifying medicines. They operate under different notions of what constitutes important proteins in biological networks. For example, proteins with high degrees of connectivity may be considered important since they can affect many neighboring proteins. The methods based on structural controllability[29-31] adopt driver genes as drug targets[24,28]. While theoretically sound and having been applied to finding cancer driver genes[25,37], this theoretically sound approach is impractical for drug repurposing as we discussed earlier. Our drug-target enrichment analysis also revealed that this approach was no better than a simple method of random selection (Figure 2E).

Our novel approach for drug repurposing stemmed from structural controllability. However, it deviated significantly from the methods that directly apply structural controllability. Instead of aiming at controlling the cell, we were motivated to protect the cell from any exogenous stimulus, particularly viral infections, because this is relatively easier than controlling the cell. Methodologically, we extended structural controllability to total controllability and exploited the former to protect the cell. We introduced control hubs to reveal the critical spots in the cell that were important for the controllability of the cell. We used targeting drugs as external influences to make the cell uncontrollable by any viral infection. Therefore, control hubs are an effective vehicle for drug repurposing, as we demonstrated in the current study on Covid-19. It is not coincident that many control hubs were also targets of existing drugs, as shown in our drug-target enrichment analysis (Figure 2E). Rather, the result revealed that proteins that have biological importance, particularly those related to immunity, resided in critical positions in the human PPI network.

To treat or prevent viral infections, control hubs in the human PPI network should be protected by blocking their interactions with viral proteins or interactions with one another which can prevent or curtail the spread of viral influence. Control hubs are thus excellent candidate drug targets for the treatment and prevention of Covid-19. The identification of such drug targets was completely data-driven and used no information on gene functions. The information on drug targets from DrugBank was brought to the analysis at a late stage of drug repurposing. Note that we used highly confident homogenous human and SARS-CoV-2 PPI data from HEK293T cells under well-controlled conditions[39-41] to avoid possible false-positive results from heterogeneous data.

Most viral proteins interacting with human proteins are nonstructural and many of them are responsible for viral transcription and replication as well as suppression of the innate and adaptive immune responses of the host (Tables S4, S7). Many druggable control hubs have immunity and antiviral related functions such as regulation of apoptotic signaling, regulation of cellular response to stress, regulation of leukocyte proliferation, and regulation of cell population proliferation (Figure 3A; Tables 1, S4). Nutrient levels are another key

exogenous factor that these control hubs responded to (Figure 3A; Tables 1, S4,). These results of druggable control hubs provided deep insight into the possible therapeutic mechanisms of the identified drugs for Covid-19 treatment (Figure 3B; Tables 2, S5), making the novel control-hub method an explainable drug repurposing approach, which is a desirable feature for repurposing drugs[26]. For example, RIPK1 interacts with viral RdRp nsp12, and CYB5R3 and COMT interact with nsp7, a cofactor of viral RdRp (Figures 2F, 2G). RIPK1 is targeted by Fostamatinib, CYB5R3 by three drugs including NADH, and COMT by 15 drugs including Conjugated estrogens (Tables 2, 3, S4A, S5). These drugs are effective for treating Covid-19, as supported by experimental and clinical data, by blocking or suppressing the transcription or replication of SARS-Cov-2 to protect the host immunity.

One of the most important results from the new method is the identification of Fostamatinib as a Covid-19 drug, particularly suitable for hospitalized patients (Figures 3C; Tables 2, S5). The functions of the ten control hubs targeted by Fostamatinib explain well the mechanistic mode of action that the medicine may perform in the treatment of severely ill Covid-19 patients. It is encouraging that this data-driven result was supported by the experimental results on a mouse model of acute lung injury and acute respiratory syndrome[64] and the data of a preliminary clinical trial on a small sample of critically ill patients[65]. Altogether, the biological functions and experimental data suggested that the drug functions prevent exaggerated autoinflammatory immune responses[129,130] and alleviate the burden of cytokine storms[131,132] in severe cases of SARS-CoV-2 infection. The large number of control hubs that Fostamatinib targets and their coherent functions strongly suggest that it is a potent drug for the disease.

A substantial number of control hubs in the 2-step community of the human PPI network are not targets of any existing drug. These control hubs can be used to propose testable hypotheses for new drug development for Covid-19 therapy. These control hubs are potentially high-quality candidates for screening small molecules for drug development. This is supported by the drug-target enrichment analysis on the druggable control hubs (Figure 2E). To make compound screening focus on Covid-19, we may focus on the control hubs that are membrane proteins and that function on the NF-κB pathway (Figure S3).

Materials and Methods

Construction of a triple-layer interaction network from viruses to humans to drugs

The core component of this multi-layer network was a human protein-protein interaction (PPI) network that was built using human binary protein interaction data from the Huri-Union dataset[39]. This is the largest homogenous human protein interactome with data collected primarily from HEK923T cells and validated in multiple orthogonal assays. The network consists of 9,092 nodes or proteins and 64,006 interactions (Table S1). Note that the Huri-Union data do not cover all proteins, including the human receptor ACE2, one of the most important proteins for studying Covid-19. To determine if ACE2 can be indeed located at a critical position among PPIs, such as a control hub, a large human PPI network was assembled using data from 21 sources, including Huri-Union[39], Interactome3D[133], Instruct[134], Insider[135], PINA[136], MINT[137], LitBM17[39], HIPPIE[138], APID[139], ENCODE consortium[139], InWeb[140], BioGrid[141], HINT[142], BioPlex[143], QUBIC[144], CoFrac[145], KinomeNetworkX[146], PhosphoSitePlus[147], SignaLink[148], and InnateDB[149]. The larger network contains 18,505 proteins and 327,924 interactions.

To expand the homogenous PPI network to include the layer of viral proteins, the SARS-CoV-2 AP-MS data[40] from HEK293T cells were added. The dataset contains 332 high-confidence virus-host interactions between 27 SARS-CoV-2 proteins and 332 human proteins. Due to the smaller size of the homogenous human PPI network, the final triple-layer network contains 169 interactions between 22 viral proteins and 169 human proteins (Table S2). The 3D Structural Interactome between SARS-CoV-2 and host proteins comes from SARS-CoV-2-Human Interactome Browser[150].

The network was further expanded to include the layer of drugs and their human protein targets using the data of drug-target associations from DrugBank[42]. Only included were drugs approved by FDA and under investigation. The drug-target interactome contains 17,780 interactions between 2,981 drugs and 2,914 target

proteins (Table S3). The information on drug categories provided by DrugBank was used to group drugs (Table S5).

Control hubs of the human PPI network

A network can be controlled by exerting control signals on *driver nodes* (Figure 1A)[29,29]. To analyze the controllability of a network, maximum matching from graph theory was adopted to find the minimum set of driver nodes[31]. A *maximum matching* is the maximum set of edges that do not share nodes in common[46]. The edges of a maximum matching form edge-independent paths of the network, which start from *head nodes*, along the matching edges, to reach tail nodes. The head nodes of a maximum matching are taken as driver nodes and the paths are referred to as *control paths*[151] (Figure 1A), which collectively constitute a *control scheme*. The maximum matching is not unique for most networks, neither is the control scheme (Figure 1A).

A node may occupy distinct positions in control paths of different control schemes. It may be a driver, a tail, or a middle node in different control schemes. Some nodes may always remain as middle nodes in all control schemes, and such nodes are defined as *control hub*s (Figure 1B). All control hubs can be identified in polynomial time without computing all control schemes[152].

Node ranking methods

Several methods are available for ranking nodes based on their connectivity and network topologies. In the sequel, a network with n nodes is considered. The degree centrality [47] of node i, $\mathrm{dc}_i = \frac{degree_i}{n-1}$, is determined by the number of neighbors connected to the node. The average neighbor degree[48] is defined as $\mathrm{nd}_i = \frac{\sum_{j\in N(i)} k_j}{|N(i)|}$, where $N(i)$ are the neighbors of node i and k_j is the degree of node j. The betweenness centrality[49] is $\mathrm{bc}_i = \sum_{s\neq i\neq t\in n} \frac{p_{s,t}(i)}{p_{s,t}}$, where $p_{s,t}(i)$ is the number of shortest paths between nodes s and t going through node i, and $p_{s,t}$ is the number of all shortest paths between nodes s and t. The load centrality is slightly different from the betweenness centrality, and can be calculated according to a method from newman[50,51]. The closeness centrality[52] is written as $\mathrm{cc}_i = \frac{r-1}{n-1}\frac{r-1}{\sum_{j=1}^{r-1} d_{i,j}}$, where $d_{i,j}$ is the length of the shortest path between nodes i and j, and r is the number of nodes reachable from node i. The Eigenvector centrality[53,54] measures the importance of a node based on the centrality of its neighbors. At convergence, it can be expressed by $\mathrm{Ax} = \lambda \mathrm{x}$, where A is the network adjacency matrix with eigenvalue λ. The clustering coefficient[153] $cl_i = \frac{2T_i}{d_i(d_i-1)}$, where T_i is the number of triangles including node i and d_i is the degree of node i. The K-core[56] of a node corresponds to the largest subnet with node degree *k* or greater. The core value of a node is the largest value k containing the node. Page rank[154,155] is a node ranking method based on network structures and is used to measure the importance of a web page relative to the other pages. All these ranking methods are available in networkx[156] and coded in python.

Identification of druggable control hubs within k-step from viral proteins and candidate drugs

To find the control hubs that were reachable within no more than *k* steps from some viral proteins, a breadth-first traversal of the triple-layer PPI network was carried out. The traversal started from the seed viral proteins and ignored edge directions. It was implemented straightforwardly by a first-in-first-out queue. The process terminated after all nodes at *k* steps from the beginning were visited.

All control hubs encountered in the process of breadth-first traversal were reported. The reported control hubs were further checked against DrugBank[42] to identify druggable control hubs.

Enrichment analysis

Let *U* be the universe and *F* the set with a feature of interest. We were interested in the enrichment of the feature for a given set *D*. For example, consider all proteins in the human PPI network that were no more than 2-steps away from viral proteins (i.e., the universe *U*) and the subset of these proteins that were drug targets

(i.e., set *F* with the feature). We were interested in the enrichment of drug targets (i.e., the feature) for the control hubs (i.e., the given set *D*). The feature enrichment of *D* can be computed as $D_F = D \cap F$. To assess the enrichment significance for D_F, a series of random sampling and a statistical test were carried out. A random sample *S* was generated by randomly drawing $|D|$ items (proteins) from *U*. $S_F = S \cap F$ was the subset of *S* with the feature of interest and a measure of feature enrichment for *S*. An empirical distribution of S_F can be derived from multiple random samplings of *S*. This empirical distribution can be taken as a baseline enrichment of the feature for items in *U*. A z-test was then adopted to evaluate the difference and significance between D and the baseline S_F. The z-test, modeled as a two-tailed Gaussian distribution, was conducted based on $Z = \frac{D_F - mean(S_F)}{SD\ of\ S_F}$, where $SD\ of\ S_F$ was the standard deviation of S_F from, say 1,000, samples. The significance of the enrichment of D_F is quantified by the *p*-value, which was from the standard normal distribution cumulative probability table.

The difference between an empirical normal distribution of S_F and another empirical normal distribution of S_F' was analyzed using the Pearson's Chi-squared test, as $\chi^2 = \sum_{i=1}^{k} \frac{(f_i - np_i)^2}{np_i}$, where k was the number of intervals; np_i was the frequency of interval i in theoretical observed distribution np (i.e., the frequency of baseline distribution S_F); f_i was the frequency of interval i in observed distribution f (as the frequency of enrichment distribution of all driver nodes). The final difference χ^2-value was calculated, and the significance *p*-value was from the Chi-square distribution table.

Gene Enrichment Analysis

To explore the biological process in which the 65 druggable control hubs were involved, functional annotation analyses with Kyoto Encyclopedia of Genes and Genomes (KEGG) pathway annotation and Gene Ontology (GO) annotation were performed using Metascape[157]. The Go BP (biological process) terms or KEGG pathways with FDR-corrected *p*-value < 0.05 were reported.

Data and Software Availability

All of the datasets used in the analysis of this study are included in Supplemental Tables S1-3. The software of our method for finding control hubs is freely available in the public software repository GitHub at https://github.com/network-control-lab/control-hubs.

Disclosure of Potential Conflicts of Interest

No potential conflicts of interest were disclosed.

Author Contributions

Weixiong Zhang and Xizhe Zhang conceived and designed the research and coordinated the project. Chunyu Pan and Xinru Wei implemented the algorithm, collected and analyzed the data, and helped with writing the manuscript and preparing the figures. Weixiong Zhang analyzed the data and draft the manuscript.

Acknowledgment

This work was supported in part by the National Natural Science Foundation of China (grant 62176129), the United States National Institutes of Health (grant R01-GM100364), and the Hong Kong Global STEM Professorship Scheme.

ORCID

Xizhe Zhang: http://orcid.org/0000-0002-8684-4591; Weixiong Zhang: http://orcid.org/0000-0002-4998-9791

Reference

1 Chan, J. F. W. *et al.* A familial cluster of pneumonia associated with the 2019 novel coronavirus indicating person-to-person transmission: a study of a family cluster. *Lancet* **395**, 514-523, doi:10.1016/s0140-6736(20)30154-9 (2020).

2 Zhou, P. *et al.* A pneumonia outbreak associated with a new coronavirus of probable bat origin. *Nature* **579**, 270-+, doi:10.1038/s41586-020-2012-7 (2020).

3 Chen, G. *et al.* Clinical and immunological features of severe and moderate coronavirus disease 2019. *The Journal of clinical investigation* **130**, 2620-2629, doi:10.1172/jci137244 (2020).

4 Huang, C. *et al.* Clinical features of patients infected with 2019 novel coronavirus in Wuhan, China. *Lancet* **395**, 497-506, doi:10.1016/s0140-6736(20)30183-5 (2020).

5 Rahmani, S. & Rezaei, N. SARS-CoV-2 Omicron variant: Why global communities should take it seriously? *Immunity, inflammation and disease* **10**, e618, doi:10.1002/iid3.618 (2022).

6 Beck, A., Goetsch, L., Dumontet, C. & Corvaïa, N. Strategies and challenges for the next generation of antibody-drug conjugates. *Nature reviews. Drug discovery* **16**, 315-337, doi:10.1038/nrd.2016.268 (2017).

7 Abd El-Aziz, T. M. & Stockand, J. D. Recent progress and challenges in drug development against COVID-19 coronavirus (SARS-CoV-2)-an update on the status. *Infection Genetics and Evolution* **83**, doi:10.1016/j.meegid.2020.104327 (2020).

8 Kim, S. COVID-19 Drug Development. *Journal of microbiology and biotechnology* **32**, 1-5, doi:10.4014/jmb.2110.10029 (2022).

9 Riva, L. *et al.* Discovery of SARS-CoV-2 antiviral drugs through large-scale compound repurposing. *Nature* **586**, 113-+, doi:10.1038/s41586-020-2577-1 (2020).

10 Guy, R. K., DiPaola, R. S., Romanelli, F. & Dutch, R. E. Rapid repurposing of drugs for COVID-19. *Science (New York, N.Y.)* **368**, 829-830, doi:10.1126/science.abb9332 (2020).

11 Ng, Y. L., Salim, C. K. & Chu, J. J. H. Drug repurposing for COVID-19: Approaches, challenges and promising candidates. *Pharmacology & therapeutics* **228**, 107930, doi:10.1016/j.pharmthera.2021.107930 (2021).

12 Yousefi, H., Mashouri, L., Okpechi, S. C., Alahari, N. & Alahari, S. K. Repurposing existing drugs for the treatment of COVID-19/SARS-CoV-2 infection: A review describing drug mechanisms of action. *Biochemical pharmacology* **183**, 114296, doi:10.1016/j.bcp.2020.114296 (2021).

13 Dotolo, S., Marabotti, A., Facchiano, A. & Tagliaferri, R. A review on drug repurposing applicable to COVID-19. *Briefings in bioinformatics* **22**, 726-741, doi:10.1093/bib/bbaa288 (2021).

14 Chakraborty, C., Sharma, A. R., Bhattacharya, M., Agoramoorthy, G. & Lee, S. S. The Drug Repurposing for COVID-19 Clinical Trials Provide Very Effective Therapeutic Combinations: Lessons Learned From Major Clinical Studies. *Front Pharmacol* **12**, 704205, doi:10.3389/fphar.2021.704205 (2021).

15 Pushpakom, S. *et al.* Drug repurposing: progress, challenges and recommendations. *Nature reviews. Drug discovery* **18**, 41-58, doi:10.1038/nrd.2018.168 (2019).

16 Martinez, M. A. What Should Be Learned From Repurposed Antivirals Against SARS-CoV-2? *Frontiers in microbiology* **13**, 843587, doi:10.3389/fmicb.2022.843587 (2022).

17 Gurung, A. B., Ali, M. A., Lee, J., Farah, M. A. & Al-Anazi, K. M. An Updated Review of Computer-Aided Drug Design and Its Application to COVID-19. *BioMed research international* **2021**, 8853056, doi:10.1155/2021/8853056 (2021).

18 Galindez, G. *et al.* Lessons from the COVID-19 pandemic for advancing computational drug repurposing strategies. *Nature Computational Science* **1**, 33-41, doi:10.1038/s43588-020-00007-6 (2021).

19 Sharma, P. P. *et al.* Computational methods directed towards drug repurposing for COVID-19: advantages and limitations. *RSC advances* **11**, 36181-36198, doi:10.1039/d1ra05320e (2021).

20 Turilli, E. S., Lualdi, M. & Fasano, M. Looking at COVID-19 from a Systems Biology Perspective. *Biomolecules* **12**, doi:10.3390/biom12020188 (2022).

21 Ge, Y. *et al.* An integrative drug repositioning framework discovered a potential therapeutic agent targeting COVID-19. *Signal transduction and targeted therapy* **6**, 165, doi:10.1038/s41392-021-00568-6 (2021).

22 Santos, S. S. *et al.* Machine learning and network medicine approaches for drug repositioning for COVID-19. *Patterns (New York, N.Y.)* **3**, 100396, doi:10.1016/j.patter.2021.100396 (2022).

23 Sadegh, S. *et al.* Exploring the SARS-CoV-2 virus-host-drug interactome for drug repurposing. *Nature communications* **11**, 3518, doi:10.1038/s41467-020-17189-2 (2020).

24 Ackerman, E. E. & Shoemaker, J. E. Network Controllability-Based Prioritization of Candidates for SARS-CoV-2 Drug Repositioning. *Viruses* **12**, doi:10.3390/v12101087 (2020).

25 Guo, W. F., Zhang, S. W., Zeng, T., Akutsu, T. & Chen, L. Network control principles for identifying personalized driver genes in cancer. *Briefings in bioinformatics* **21**, 1641-1662, doi:10.1093/bib/bbz089 (2020).

26 Jimenez-Luna, J., Grisoni, F. & Schneider, G. Drug discovery with explainable artificial intelligence. *Nature Machine Intelligence* **2**, 573-584, doi:10.1038/s42256-020-00236-4 (2020).

27 Morselli Gysi, D. *et al.* Network medicine framework for identifying drug-repurposing opportunities for COVID-19. *Proceedings of the National Academy of Sciences of the United States of America* **118**, doi:10.1073/pnas.2025581118 (2021).

28 Siminea, N. *et al.* Network analytics for drug repurposing in COVID-19. *Briefings in bioinformatics* **23**, doi:10.1093/bib/bbab490 (2022).

29 Lin, C.-T. Structural controllability. *IEEE Transactions on Automatic Control* **19**, 201-208 (1974).

30 Glover, K. & Silverman, L. Characterization of structural controllability. *IEEE Transactions on Automatic control* **21**, 534-537 (1976).

31 Liu, Y. Y., Slotine, J. J. & Barabási, A. L. Controllability of complex networks. *Nature* **473**, 167-173, doi:10.1038/nature10011 (2011).

32 Kanhaiya, K., Czeizler, E., Gratie, C. & Petre, I. Controlling Directed Protein Interaction Networks in Cancer. *Scientific reports* **7**, 10327, doi:10.1038/s41598-017-10491-y (2017).

33 Qian, X., Ivanov, I., Ghaffari, N. & Dougherty, E. R. Intervention in gene regulatory networks via greedy control policies based on long-run behavior. *BMC systems biology* **3**, 61, doi:10.1186/1752-0509-3-61 (2009).

34 Bolouri, H. *Computational modeling of gene regulatory networks-a primer*. (World Scientific Publishing Company, 2008).

35 Asgari, Y., Salehzadeh-Yazdi, A., Schreiber, F. & Masoudi-Nejad, A. Controllability in cancer metabolic networks according to drug targets as driver nodes. *PloS one* **8**, e79397, doi:10.1371/journal.pone.0079397 (2013).

36 Bailey, M. H. *et al.* Comprehensive Characterization of Cancer Driver Genes and Mutations. *Cell* **173**, 371-385.e318, doi:10.1016/j.cell.2018.02.060 (2018).

37 Guo, W. F. *et al.* Network controllability-based algorithm to target personalized driver genes for discovering combinatorial drugs of individual patients. *Nucleic acids research* **49**, e37, doi:10.1093/nar/gkaa1272 (2021).

38 Valiant, L. G. The complexity of computing the permanent. *Theoretical computer science* **8**, 189-201 (1979).

39 Luck, K. *et al.* A reference map of the human binary protein interactome. *Nature* **580**, 402-408, doi:10.1038/s41586-020-2188-x (2020).

40 Gordon, D. E. *et al.* A SARS-CoV-2 protein interaction map reveals targets for drug repurposing. *Nature* **583**, 459-468, doi:10.1038/s41586-020-2286-9 (2020).

41 Gordon, D. E. *et al.* Comparative host-coronavirus protein interaction networks reveal pan-viral disease mechanisms. *Science (New York, N.Y.)* **370**, doi:10.1126/science.abe9403 (2020).

42 Wishart, D. S. *et al.* DrugBank: a knowledgebase for drugs, drug actions and drug targets. *Nucleic acids research* **36**, D901-906, doi:10.1093/nar/gkm958 (2008).

43 Li, F. Structure, Function, and Evolution of Coronavirus Spike Proteins. *Annual review of virology* **3**, 237-261, doi:10.1146/annurev-virology-110615-042301 (2016).

44 Hoffmann, M. *et al.* SARS-CoV-2 Cell Entry Depends on ACE2 and TMPRSS2 and Is Blocked by a Clinically Proven Protease Inhibitor. *Cell* **181**, 271-280.e278, doi:10.1016/j.cell.2020.02.052 (2020).

45 Li, J., Zhan, P. & Liu, X. Targeting the entry step of SARS-CoV-2: a promising therapeutic approach. *Signal transduction and targeted therapy* **5**, 98, doi:10.1038/s41392-020-0195-x (2020).

46 Hopcroft, J. E. & Karp, R. M. An n^5/2 algorithm for maximum matchings in bipartite graphs. *SIAM Journal on computing* **2**, 225-231 (1973).

47 Borgatti, S. P. & Halgin, D. S. Analyzing affiliation networks. *The Sage handbook of social network analysis* **1**, 417-433 (2011).

48 Barrat, A., Barthelemy, M., Pastor-Satorras, R. & Vespignani, A. The architecture of complex weighted networks. *Proceedings of the national academy of sciences* **101**, 3747-3752 (2004).

49 Brandes, U. On variants of shortest-path betweenness centrality and their generic computation. *Social networks* **30**, 136-145 (2008).

50 Newman, M. E. Scientific collaboration networks. II. Shortest paths, weighted networks, and centrality. *Physical review E* **64**, 016132 (2001).

51 Goh, K.-I., Kahng, B. & Kim, D. Universal behavior of load distribution in scale-free networks. *Physical review letters* **87**, 278701 (2001).

52 Freeman, L. Centrality in networks: I. conceptual clarifications. social networks. *Social Network* (1979).

53 Bonacich, P. Power and centrality: A family of measures. *American journal of sociology* **92**, 1170-1182 (1987).

54 Brede, M. Networks—An Introduction. Mark EJ Newman, (MIT Press One Rogers Street, Cambridge, MA 02142-1209, USA journals-info …, 2012).

55 Zhang, J.-X., Chen, D.-B., Dong, Q. & Zhao, Z.-D. Identifying a set of influential spreaders in complex networks. **6**, 1-10 (2016).

56 Batagelj, V. & Zaversnik, M. An O (m) algorithm for cores decomposition of networks. *arXiv preprint cs/0310049* (2003).

57 Gao, Y. *et al.* Structure of the RNA-dependent RNA polymerase from COVID-19 virus. *Science (New York, N.Y.)* **368**, 779-782, doi:10.1126/science.abb7498 (2020).

58 Wang, W. *et al.* SARS-CoV-2 nsp12 attenuates type I interferon production by inhibiting IRF3 nuclear translocation. *Cellular & molecular immunology* **18**, 945-953, doi:10.1038/s41423-020-00619-y (2021).

59 Zhang, C., Li, L., He, J., Chen, C. & Su, D. Nonstructural protein 7 and 8 complexes of SARS-CoV-2. *Protein science : a publication of the Protein Society* **30**, 873-881, doi:10.1002/pro.4046 (2021).

60 Mifflin, L., Ofengeim, D. & Yuan, J. Receptor-interacting protein kinase 1 (RIPK1) as a therapeutic target. *Nature reviews. Drug discovery* **19**, 553-571, doi:10.1038/s41573-020-0071-y (2020).

61 Yuan, J., Amin, P. & Ofengeim, D. Necroptosis and RIPK1-mediated neuroinflammation in CNS diseases. *Nature reviews. Neuroscience* **20**, 19-33, doi:10.1038/s41583-018-0093-1 (2019).

62 Xu, G. *et al.* SARS-CoV-2 promotes RIPK1 activation to facilitate viral propagation. *Cell research* **31**, 1230-1243, doi:10.1038/s41422-021-00578-7 (2021).

63 Strich, J. R. *et al.* Fostamatinib Inhibits Neutrophils Extracellular Traps Induced by COVID-19 Patient Plasma: A Potential Therapeutic. *The Journal of infectious diseases* **223**, 981-984, doi:10.1093/infdis/jiaa789 (2021).

64 Kost-Alimova, M. *et al.* A High-Content Screen for Mucin-1-Reducing Compounds Identifies Fostamatinib as a Candidate for Rapid Repurposing for Acute Lung Injury. *Cell reports. Medicine* **1**, 100137, doi:10.1016/j.xcrm.2020.100137 (2020).

65 Strich, J. R. *et al.* Fostamatinib for the treatment of hospitalized adults with COVD-19 A randomized trial. *Clinical infectious diseases : an official publication of the Infectious Diseases Society of America*, doi:10.1093/cid/ciab732 (2021).

66 Hoepel, W. *et al.* High titers and low fucosylation of early human anti-SARS-CoV-2 IgG promote inflammation by alveolar macrophages. *Science translational medicine* **13**, doi:10.1126/scitranslmed.abf8654 (2021).

67 Apostolidis, S. A. *et al.* Signaling through FcγRIIA and the C5a-C5aR pathway mediates platelet hyperactivation in COVID-19. *bioRxiv : the preprint server for biology*, doi:10.1101/2021.05.01.442279 (2021).

68 Rivero-García, I., Castresana-Aguirre, M., Guglielmo, L., Guala, D. & Sonnhammer, E. L. L. Drug repurposing improves disease targeting 11-fold and can be augmented by network module targeting, applied to COVID-19. *Scientific reports* **11**, 20687, doi:10.1038/s41598-021-99721-y (2021).

69 Brenner, C. Viral infection as an NAD(+) battlefield. *Nature metabolism* **4**, 2-3, doi:10.1038/s42255-021-00507-3 (2022).

70 Heer, C. D. *et al.* Coronavirus infection and PARP expression dysregulate the NAD metabolome: An actionable component of innate immunity. *The Journal of biological chemistry* **295**, 17986-17996, doi:10.1074/jbc.RA120.015138 (2020).

71 Altay, O. *et al.* Combined Metabolic Activators Accelerates Recovery in Mild-to-Moderate COVID-19. *Advanced Science* **8**, doi:10.1002/advs.202101222 (2021).

72 Brandi, M. L. Are sex hormones promising candidates to explain sex disparities in the COVID-19 pandemic? *Reviews in endocrine & metabolic disorders* **23**, 171-183, doi:10.1007/s11154-021-09692-8 (2022).

73 Chen, N. *et al.* Epidemiological and clinical characteristics of 99 cases of 2019 novel coronavirus pneumonia in Wuhan, China: a descriptive study. *Lancet* **395**, 507-513, doi:10.1016/s0140-6736(20)30211-7 (2020).

74 Guan, W. J. *et al.* Clinical Characteristics of Coronavirus Disease 2019 in China. *The New England journal of medicine* **382**, 1708-1720, doi:10.1056/NEJMoa2002032 (2020).

75 Channappanavar, R. *et al.* Sex-Based Differences in Susceptibility to Severe Acute Respiratory Syndrome Coronavirus Infection. *Journal of immunology (Baltimore, Md. : 1950)* **198**, 4046-4053, doi:10.4049/jimmunol.1601896 (2017).

76 Yan, H. *et al.* Sodium taurocholate cotransporting polypeptide is a functional receptor for human hepatitis B and D virus. *eLife* **1**, e00049, doi:10.7554/eLife.00049 (2012).

77 Ghandehari, S. *et al.* Progesterone in Addition to Standard of Care vs Standard of Care Alone in the Treatment of Men Hospitalized With Moderate to Severe COVID-19: A Randomized, Controlled Pilot Trial. *Chest* **160**, 74-84, doi:10.1016/j.chest.2021.02.024 (2021).

78 Shah, S. B. COVID-19 and Progesterone: Part 1. SARS-CoV-2, Progesterone and its potential clinical use. *Endocrine and metabolic science* **5**, 100109, doi:10.1016/j.endmts.2021.100109 (2021).

79 Ravichandran, R. *et al.* An open label randomized clinical trial of Indomethacin for mild and moderate hospitalised Covid-19 patients. *Scientific reports* **12**, 6413, doi:10.1038/s41598-022-10370-1 (2022).

80 Shekhar, N., Kaur, H., Sarma, P., Prakash, A. & Medhi, B. Indomethacin: an exploratory study of antiviral mechanism and host-pathogen interaction in COVID-19. *Expert review of anti-infective therapy* **20**, 383-390, doi:10.1080/14787210.2022.1990756 (2022).

81 Pizzorno, A. *et al.* In vitro evaluation of antiviral activity of single and combined repurposable drugs against SARS-CoV-2. *Antiviral research* **181**, 104878, doi:10.1016/j.antiviral.2020.104878 (2020).

82 Softic, L. *et al.* Inhibition of SARS-CoV-2 Infection by the Cyclophilin Inhibitor Alisporivir (Debio 025). *Antimicrobial agents and chemotherapy* **64**, doi:10.1128/aac.00876-20 (2020).

83 Ogando, N. S. *et al.* SARS-coronavirus-2 replication in Vero E6 cells: replication kinetics, rapid adaptation and cytopathology. *The Journal of general virology* **101**, 925-940, doi:10.1099/jgv.0.001453 (2020).

84 Devaux, C. A., Melenotte, C., Piercecchi-Marti, M. D., Delteil, C. & Raoult, D. Cyclosporin A: A Repurposable Drug in the Treatment of COVID-19? *Frontiers in medicine* **8**, 663708, doi:10.3389/fmed.2021.663708 (2021).

85 Tomo, S., Banerjee, M., Sharma, P. & Garg, M. Does dehydroepiandrosterone sulfate have a role in COVID-19 prognosis and treatment? *Endocrine regulations* **55**, 174-181, doi:10.2478/enr-2021-0019 (2021).

86 Pinna, G. Sex and COVID-19: A Protective Role for Reproductive Steroids. *Trends in endocrinology and metabolism: TEM* **32**, 3-6, doi:10.1016/j.tem.2020.11.004 (2021).

87 Kuzmich, N. N. *et al.* TLR4 Signaling Pathway Modulators as Potential Therapeutics in Inflammation and Sepsis. *Vaccines* **5**, doi:10.3390/vaccines5040034 (2017).

88 Beishuizen, A., Thijs, L. G. & Vermes, I. Decreased levels of dehydroepiandrosterone sulphate in severe critical illness: a sign of exhausted adrenal reserve? *Critical care (London, England)* **6**, 434-438, doi:10.1186/cc1530 (2002).

89 Cutolo, M., Foppiani, L. & Minuto, F. Hypothalamic-pituitary-adrenal axis impairment in the pathogenesis of rheumatoid arthritis and polymyalgia rheumatica. *Journal of endocrinological investigation* **25**, 19-23 (2002).

90 Kato, K., Lillehoj, E. P., Lu, W. & Kim, K. C. MUC1: The First Respiratory Mucin with an Anti-Inflammatory Function. *Journal of clinical medicine* **6**, doi:10.3390/jcm6120110 (2017).

91 Nakashima, T. *et al.* Circulating KL-6/MUC1 as an independent predictor for disseminated intravascular coagulation in acute respiratory distress syndrome. *Journal of internal medicine* **263**, 432-439, doi:10.1111/j.1365-2796.2008.01929.x (2008).

92 Ruan, Q., Yang, K., Wang, W., Jiang, L. & Song, J. Clinical predictors of mortality due to COVID-19 based on an analysis of data of 150 patients from Wuhan, China. *Intensive care medicine* **46**, 846-848, doi:10.1007/s00134-020-05991-x (2020).

93 Zhou, F. *et al.* Clinical course and risk factors for mortality of adult inpatients with COVID-19 in Wuhan, China: a retrospective cohort study. *Lancet* **395**, 1054-1062, doi:10.1016/s0140-6736(20)30566-3 (2020).

94 Ostojic, S. M., Milovancev, A., Drid, P. & Nikolaidis, A. Oxygen saturation improved with nitrate-based nutritional formula in patients with COVID-19. *The Journal of international medical research* **49**, 3000605211012380, doi:10.1177/03000605211012380 (2021).

95 Jovic, T. H. *et al.* Could Vitamins Help in the Fight Against COVID-19? *Nutrients* **12**, doi:10.3390/nu12092550 (2020).

96 Meydani, S. N. *et al.* Vitamin E and respiratory tract infections in elderly nursing home residents: a randomized controlled trial. *Jama* **292**, 828-836, doi:10.1001/jama.292.7.828 (2004).

97 Samad, N. *et al.* Fat-Soluble Vitamins and the Current Global Pandemic of COVID-19: Evidence-Based Efficacy from Literature Review. *Journal of inflammation research* **14**, 2091-2110, doi:10.2147/jir.S307333 (2021).

98 Beigmohammadi, M. T. *et al.* The effect of supplementation with vitamins A, B, C, D, and E on disease severity and inflammatory responses in patients with COVID-19: a randomized clinical trial. *Trials* **22**, 802, doi:10.1186/s13063-021-05795-4 (2021).

99 Mutua, V. & Gershwin, L. J. A Review of Neutrophil Extracellular Traps (NETs) in Disease: Potential Anti-NETs Therapeutics. *Clinical reviews in allergy & immunology* **61**, 194-211, doi:10.1007/s12016-020-08804-7 (2021).

100 Middleton, E. A. *et al.* Neutrophil extracellular traps contribute to immunothrombosis in COVID-19 acute respiratory distress syndrome. *Blood* **136**, 1169-1179, doi:10.1182/blood.2020007008 (2020).

101 Bautista-Becerril, B. *et al.* Immunothrombosis in COVID-19: Implications of Neutrophil Extracellular Traps. *Biomolecules* **11**, doi:10.3390/biom11050694 (2021).

102 Szturmowicz, M. & Demkow, U. Neutrophil Extracellular Traps (NETs) in Severe SARS-CoV-2 Lung Disease. *International journal of molecular sciences* **22**, doi:10.3390/ijms22168854 (2021).

103 Capra, M. *et al.* Frequent alterations in the expression of serine/threonine kinases in human cancers. *Cancer research* **66**, 8147-8154, doi:10.1158/0008-5472.Can-05-3489 (2006).

104 Torres, B. *et al.* Impact of low serum calcium at hospital admission on SARS-CoV-2 infection outcome. *International journal of infectious diseases : IJID : official publication of the International Society for Infectious Diseases* **104**, 164-168, doi:10.1016/j.ijid.2020.11.207 (2021).

105 Alemzadeh, E., Alemzadeh, E., Ziaee, M., Abedi, A. & Salehiniya, H. The effect of low serum calcium level on the severity and mortality of Covid patients: A systematic review and meta-analysis. *Immunity, inflammation and disease* **9**, 1219-1228, doi:10.1002/iid3.528 (2021).

106 Pechlivanidou, E. *et al.* The prognostic role of micronutrient status and supplements in COVID-19 outcomes: A systematic review. *Food and chemical toxicology : an international journal published for the British Industrial Biological Research Association* **162**, 112901, doi:10.1016/j.fct.2022.112901 (2022).

107 Gusev, E., Sarapultsev, A., Solomatina, L. & Chereshnev, V. SARS-CoV-2-Specific Immune Response and the Pathogenesis of COVID-19. *International journal of molecular sciences* **23**, doi:10.3390/ijms23031716 (2022).

108 Wrapp, D. *et al.* Cryo-EM structure of the 2019-nCoV spike in the prefusion conformation. *Science (New York, N.Y.)* **367**, 1260-1263, doi:10.1126/science.abb2507 (2020).

109 Zou, X. *et al.* Single-cell RNA-seq data analysis on the receptor ACE2 expression reveals the potential risk of different human organs vulnerable to 2019-nCoV infection. *Frontiers of medicine* **14**, 185-192, doi:10.1007/s11684-020-0754-0 (2020).

110 Hamming, I. *et al.* Tissue distribution of ACE2 protein, the functional receptor for SARS coronavirus. A first step in understanding SARS pathogenesis. *The Journal of pathology* **203**, 631-637, doi:10.1002/path.1570 (2004).

111 Ansarin, K. *et al.* Effect of bromhexine on clinical outcomes and mortality in COVID-19 patients: A randomized clinical trial. *BioImpacts : BI* **10**, 209-215, doi:10.34172/bi.2020.27 (2020).

112 Mikhaylov, E. N. *et al.* Bromhexine Hydrochloride Prophylaxis of COVID-19 for Medical Personnel: A Randomized Open-Label Study. *Interdisciplinary perspectives on infectious diseases* **2022**, 4693121, doi:10.1155/2022/4693121 (2022).

113 Kamel, A. M., Monem, M. S. A., Sharaf, N. A., Magdy, N. & Farid, S. F. Efficacy and safety of azithromycin in Covid-19 patients: A systematic review and meta-analysis of randomized clinical trials. *Reviews in medical virology* **32**, e2258, doi:10.1002/rmv.2258 (2022).

114 Cavalcanti, A. B. *et al.* Hydroxychloroquine with or without Azithromycin in Mild-to-Moderate Covid-19. *The New England journal of medicine* **383**, 2041-2052, doi:10.1056/NEJMoa2019014 (2020).

115 Lane, J. C. E. *et al.* Risk of hydroxychloroquine alone and in combination with azithromycin in the treatment of rheumatoid arthritis: a multinational, retrospective study. *The Lancet. Rheumatology* **2**, e698-e711, doi:10.1016/s2665-9913(20)30276-9 (2020).

116 Gu, Y. *et al.* Receptome profiling identifies KREMEN1 and ASGR1 as alternative functional receptors of SARS-CoV-2. *Cell research* **32**, 24-37, doi:10.1038/s41422-021-00595-6 (2022).

117 Twarda-Clapa, A., Olczak, A., Białkowska, A. M. & Koziołkiewicz, M. Advanced Glycation End-Products (AGEs): Formation, Chemistry, Classification, Receptors, and Diseases Related to AGEs. *Cells* **11**, doi:10.3390/cells11081312 (2022).

118 Sun, J. K. *et al.* Serum calcium as a biomarker of clinical severity and prognosis in patients with coronavirus disease 2019. *Aging* **12**, 11287-11295, doi:10.18632/aging.103526 (2020).

119 Forman, H. J., Zhang, H. & Rinna, A. Glutathione: overview of its protective roles, measurement, and biosynthesis. *Molecular aspects of medicine* **30**, 1-12, doi:10.1016/j.mam.2008.08.006 (2009).

120 De Flora, S., Grassi, C. & Carati, L. Attenuation of influenza-like symptomatology and improvement of cell-mediated immunity with long-term N-acetylcysteine treatment. *The European respiratory journal* **10**, 1535-1541, doi:10.1183/09031936.97.10071535 (1997).

121 Horowitz, R. I., Freeman, P. R. & Bruzzese, J. Efficacy of glutathione therapy in relieving dyspnea associated with COVID-19 pneumonia: A report of 2 cases. *Respiratory medicine case reports* **30**, 101063, doi:10.1016/j.rmcr.2020.101063 (2020).

122 DiNicolantonio, J. J. & O'Keefe, J. H. Magnesium and Vitamin D Deficiency as a Potential Cause of Immune Dysfunction, Cytokine Storm and Disseminated Intravascular Coagulation in covid-19 patients. *Missouri medicine* **118**, 68-73 (2021).

123 Alnafiey, M. O., Alangari, A. M., Alarifi, A. M. & Abushara, A. Persistent Hypokalemia post SARS-coV-2 infection, is it a life-long complication? Case report. *Annals of medicine and surgery (2012)* **62**, 358-361, doi:10.1016/j.amsu.2021.01.049 (2021).

124 Tam, M., Gómez, S., González-Gross, M. & Marcos, A. Possible roles of magnesium on the immune system. *European journal of clinical nutrition* **57**, 1193-1197, doi:10.1038/sj.ejcn.1601689 (2003).

125 Causton, H. C. SARS-CoV2 Infection and the Importance of Potassium Balance. *Frontiers in medicine* **8**, 744697-744697, doi:10.3389/fmed.2021.744697 (2021).

126 Hachem, H. *et al.* Rapid and sustained decline in CXCL-10 (IP-10) annotates clinical outcomes following TNF-α antagonist therapy in hospitalized patients with severe and critical COVID-19 respiratory failure. *medRxiv : the preprint server for health sciences*, doi:10.1101/2021.05.29.21258010 (2021).

127 Muley, V. Y., Singh, A., Gruber, K. & Varela-Echavarría, A. SARS-CoV-2 Entry Protein TMPRSS2 and Its Homologue, TMPRSS4 Adopts Structural Fold Similar to Blood Coagulation and Complement Pathway Related Proteins. *bioRxiv : the preprint server for biology* (2021).

128 Zang, R. *et al.* TMPRSS2 and TMPRSS4 promote SARS-CoV-2 infection of human small intestinal enterocytes. *Science immunology* **5**, doi:10.1126/sciimmunol.abc3582 (2020).

129 Tan, L. Y., Komarasamy, T. V. & Rmt Balasubramaniam, V. Hyperinflammatory Immune Response and COVID-19: A Double Edged Sword. *Frontiers in immunology* **12**, 742941, doi:10.3389/fimmu.2021.742941 (2021).

130 Rodríguez, Y. *et al.* Autoinflammatory and autoimmune conditions at the crossroad of COVID-19. *Journal of autoimmunity* **114**, 102506, doi:10.1016/j.jaut.2020.102506 (2020).

131 Hu, B., Huang, S. & Yin, L. The cytokine storm and COVID-19. *Journal of medical virology* **93**, 250-256, doi:10.1002/jmv.26232 (2021).

132 Jiang, Y. *et al.* Cytokine storm in COVID-19: from viral infection to immune responses, diagnosis and therapy. *International journal of biological sciences* **18**, 459-472, doi:10.7150/ijbs.59272 (2022).

133 Mosca, R., Céol, A. & Aloy, P. Interactome3D: adding structural details to protein networks. *Nature methods* **10**, 47-53, doi:10.1038/nmeth.2289 (2013).

134 Meyer, M. J., Das, J., Wang, X. & Yu, H. INstruct: a database of high-quality 3D structurally resolved protein interactome networks. *Bioinformatics (Oxford, England)* **29**, 1577-1579, doi:10.1093/bioinformatics/btt181 (2013).

135 Meyer, M. J. *et al.* Interactome INSIDER: a structural interactome browser for genomic studies. *Nature methods* **15**, 107-114, doi:10.1038/nmeth.4540 (2018).

136 Cowley, M. J. *et al.* PINA v2.0: mining interactome modules. *Nucleic acids research* **40**, D862-865, doi:10.1093/nar/gkr967 (2012).

137 Licata, L. *et al.* MINT, the molecular interaction database: 2012 update. *Nucleic acids research* **40**, D857-861, doi:10.1093/nar/gkr930 (2012).

138 Alanis-Lobato, G., Andrade-Navarro, M. A. & Schaefer, M. H. HIPPIE v2.0: enhancing meaningfulness and reliability of protein-protein interaction networks. *Nucleic acids research* **45**, D408-d414, doi:10.1093/nar/gkw985 (2017).

139 Alonso-López, D. *et al.* APID database: redefining protein-protein interaction experimental evidences and binary interactomes. *Database : the journal of biological databases and curation* **2019**, doi:10.1093/database/baz005 (2019).

140 Li, T. *et al.* A scored human protein-protein interaction network to catalyze genomic interpretation. *Nature methods* **14**, 61-64, doi:10.1038/nmeth.4083 (2017).

141 Chatr-Aryamontri, A. *et al.* The BioGRID interaction database: 2017 update. *Nucleic acids research* **45**, D369-d379, doi:10.1093/nar/gkw1102 (2017).

142 Das, J. & Yu, H. HINT: High-quality protein interactomes and their applications in understanding human disease. *BMC systems biology* **6**, 92, doi:10.1186/1752-0509-6-92 (2012).

143 Huttlin, E. L. *et al.* Architecture of the human interactome defines protein communities and disease networks. *Nature* **545**, 505-509, doi:10.1038/nature22366 (2017).

144 Hein, M. Y. *et al.* A human interactome in three quantitative dimensions organized by stoichiometries and abundances. *Cell* **163**, 712-723, doi:10.1016/j.cell.2015.09.053 (2015).

145 Wan, C. *et al.* Panorama of ancient metazoan macromolecular complexes. *Nature* **525**, 339-344, doi:10.1038/nature14877 (2015).

146 Cheng, F., Jia, P., Wang, Q. & Zhao, Z. Quantitative network mapping of the human kinome interactome reveals new clues for rational kinase inhibitor discovery and individualized cancer therapy. *Oncotarget* **5**, 3697-3710, doi:10.18632/oncotarget.1984 (2014).

147 Hornbeck, P. V. *et al.* PhosphoSitePlus, 2014: mutations, PTMs and recalibrations. *Nucleic acids research* **43**, D512-520, doi:10.1093/nar/gku1267 (2015).

148 Fazekas, D. *et al.* SignaLink 2 - a signaling pathway resource with multi-layered regulatory networks. *BMC systems biology* **7**, 7, doi:10.1186/1752-0509-7-7 (2013).

149 Breuer, K. *et al.* InnateDB: systems biology of innate immunity and beyond--recent updates and continuing curation. *Nucleic acids research* **41**, D1228-1233, doi:10.1093/nar/gks1147 (2013).

150 Wierbowski, S. D. *et al.* A 3D Structural Interactome to Explore the Impact of Evolutionary Divergence, Population Variation, and Small-molecule Drugs on SARS-CoV-2-Human Protein-Protein Interactions. *bioRxiv : the preprint server for biology*, 2020.10.13.308676, doi:10.1101/2020.10.13.308676 (2020).

151 Ruths, J. & Ruths, D. Control profiles of complex networks. *Science (New York, N.Y.)* **343**, 1373-1376, doi:10.1126/science.1242063 (2014).

152 Zhang, X., Pan, C. & Zhang, W. Control hubs of complex networks and a polynomial-time identification algorithm. arXiv:2206.01188 (2022). doi: 10.48550/arXiv.2206.01188.

153 Saramäki, J., Kivelä, M., Onnela, J.-P., Kaski, K. & Kertesz, J. J. P. R. E. Generalizations of the clustering coefficient to weighted complex networks. **75**, 027105 (2007).

154 Langville, A. N. & Meyer, C. D. A survey of eigenvector methods for web information retrieval. *SIAM review* **47**, 135-161 (2005).

155 Page, L., Brin, S., Motwani, R. & Winograd, T. The PageRank citation ranking: Bringing order to the web. (Stanford InfoLab, 1999).

156 Hagberg, A., Swart, P. & S Chult, D. Exploring network structure, dynamics, and function using NetworkX. (Los Alamos National Lab.(LANL), Los Alamos, NM (United States), 2008).

157 Zhou, Y. *et al.* Metascape provides a biologist-oriented resource for the analysis of systems-level datasets. *Nature communications* **10**, 1-10 (2019).

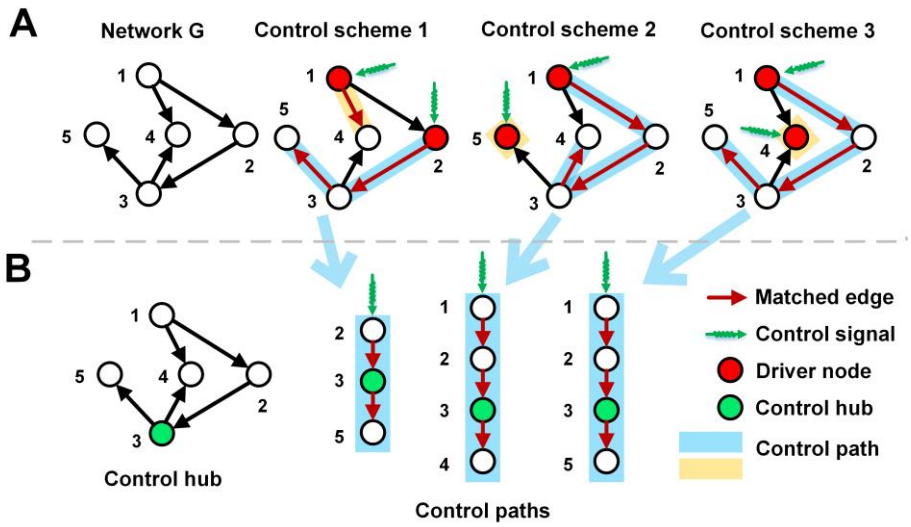

Figure 1 | All control schemes and control hubs of a small network *G*. **A)** Three distinct control schemes are identified by the maximum matching of *G*. Starting from a driver node (in red), a control path follows matched edges (in red). All control paths form a control scheme for *G*, and *G* has three control schemes. **B)** *G* has one control hub node (in green), which appears in the middle of a control path of each of the three control schemes.

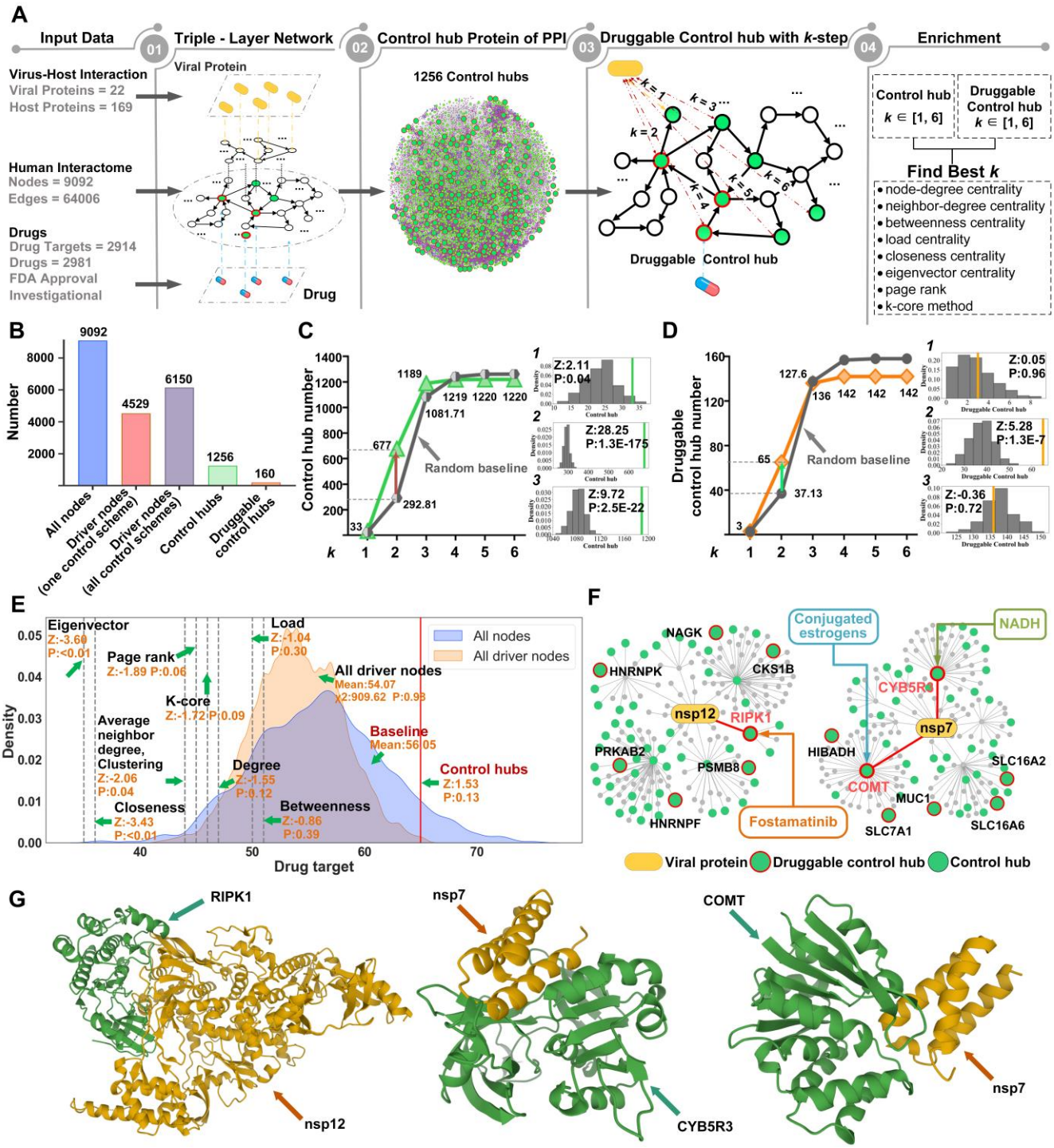

Figure 2 | Identification and characterization of druggable control hubs for blocking SARS-Cov-2 in the human PPI network. **A)** The study design and the framework of the new control-hub-based approach. A triple-layer network, connecting the viral and human proteins as well as drugs and human protein targets. The study focused on the community of proteins that were no more than 2 steps away from viral proteins (i.e., the 2-step community) and the 65 druggable control hubs within the community. The enrichment of druggable control hubs within the 2-step community was assessed against that of several gene ranking methods (see main text). **B)** Distributions of the driver nodes, control hubs, and druggable control hubs in the human PPI network. **C)** Determine that the 2-step community was most enriched with control hubs among all such communities of proteins with different *k* steps away from viral proteins. Statistical analysis was adopted to compare the

number of control hubs (in green) within a community against a random empirical distribution (i.e., the baseline in grey, also three small, inserted figures). The highest increment of control hubs from the baseline occurred at *k*=2. **D)** The 2-step community was also enriched with druggable control hubs. The same statistical analysis as in C) was performed. **E)** Comparison of drug-target enrichment of the new method and that of the driver-node method and several node ranking methods in the 2-step community. **F)** Network topologies of two SARS-Cov-2 proteins (nsp12 and nsp7 that are responsible for viral transcription and replication) and three human proteins (RIPK1, COMT, and CYB5R3) that directly interact with nsp12 and nsp7. **G)** The binding structures of two SARS-Cov-2 proteins (nsp12 and nsp7) and three druggable control hubs (RIPK1, COMT, and CYB5R3).

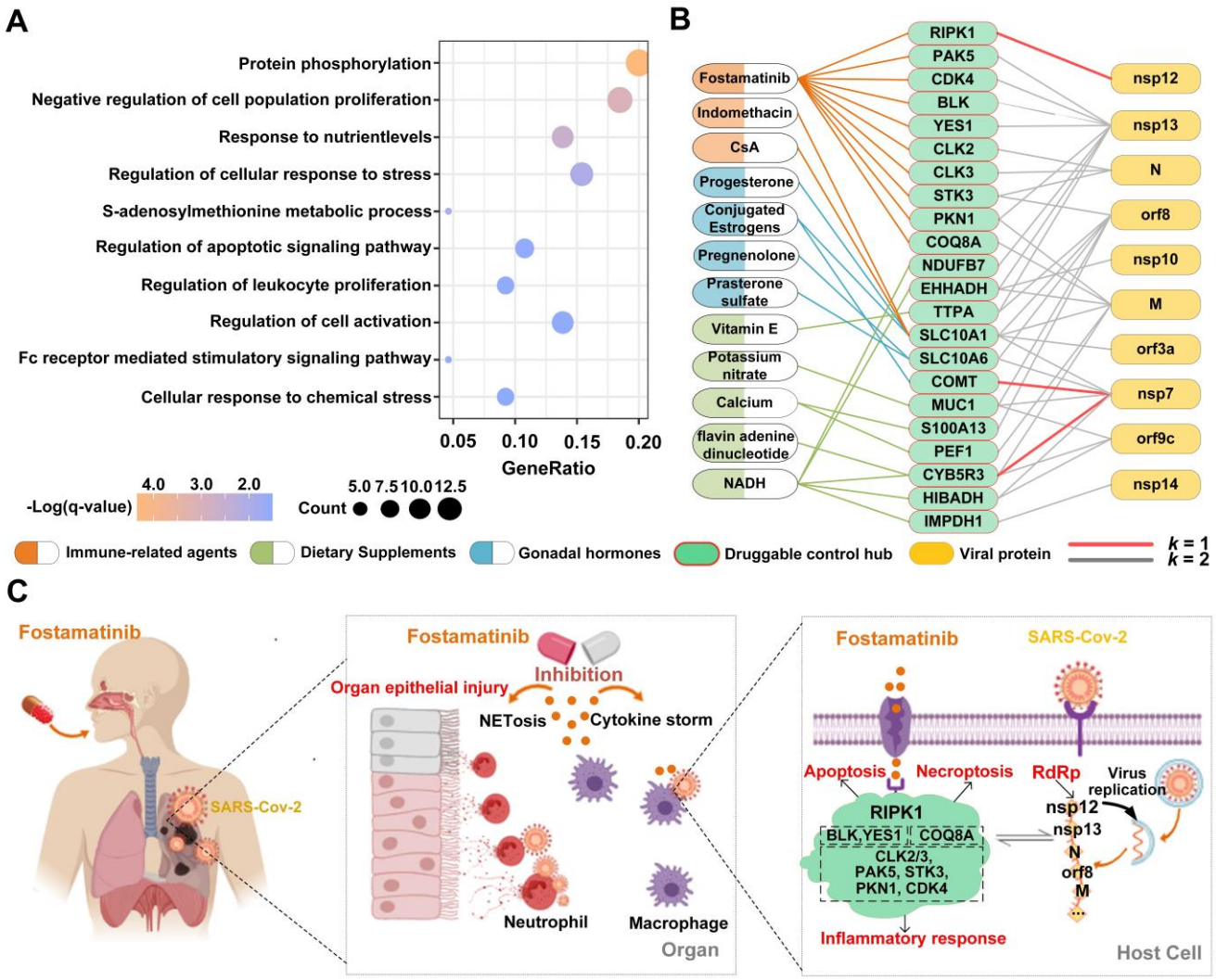

Figure 3 | Potential therapeutic mechanisms of some druggable control hubs and some selected drugs for treatment and/or prevention of Covid-19. **A)** The biological-process enrichment of the 65 druggable control hubs within the 2-step community, revealing their collective functions during viral infection. GeneRatio is the ratio between the number of observed proteins and the number of expected proteins with a specific Go term. **B)** The interactions among SARS-Cov-2 proteins, key druggable control hubs, and drugs in three categories. Drugs are grouped based on their functions, marked in color. The drugs in orange correspond to immune-related agents, such as antineoplastic or Immunomodulating agents, in green are dietary supplements, such as Vitamins and Calcium, and in blue are gonadal hormones. **C)** The potential therapeutic mechanisms of Fostamatinib for treating Covid-19. It reduces excessive immune and autoinflammatory responses by targeting 10 control hubs, 9 of which are protein kinases and one on the p53 pathway.

Table 1 | Twenty-eight of the 65 druggable control hubs (in Table S4) within no more than two steps away from SARS-Cov-2 proteins in the triple-layer PPI network. Shown are the druggable control hub (the **Host Protein** column), engaging **Viral Protein** (and the [**Distance**] between the host and viral proteins), **Host Protein Function**, and **Targeting Drugs** (and the **Total number** of drugs targeting the protein). Drugs are grouped based on their function categories marked in color. Drugs in orange correspond to immune-related agents, in green are dietary supplements, and in blue are gonadal hormones. The seven druggable control hubs discussed in the text are marked in grey background. The rest 21 druggable control hubs are targeted by at least two drugs.

Host Protein	Viral Protein [Distance]	Host Protein Function	Targeting Drugs (Total number)
RIPK1	nsp12[1]	Inflammation, cell death, pathogen recognition	Fostamatinib
CYB5R3	nsp7[1], orf9c[2], M[2]	Cholesterol biosynthetic process.	NADH, Flavin adenine dinucleotide, Copper
COMT	nsp7[1]	Neurotransmitter catabolic process	Conjugated estrogens, Diethylstilbestrol, Tolcapone (15)
SLC10A1	nsp7[2], orf8[2], orf3a[2], M[2]	Bile acid and bile salt transport	Conjugated estrogens, Progesterone, Indomethacin, Cyclosporine A (CsA) (18)
SLC10A6	nsp7[2], orf8[2]	Transmembrane transport	Pregnenolone, Prasterone sulfate
MUC1	nsp7[2], orf9c[2], orf8[2]	Forming protective mucous barriers on epithelial surfaces	Fostamatinib, Potassium nitrate, TG4010
TTPA	orf8[2], nsp13[2]	Vitamin E metabolic process	Vitamin E supplements (6)
OPRM1	orf8[2]	A class of opioid receptors	Tramadol, Morphine, Codeine (47)
TSPO	orf8[2]	Steroid hormone synthesis, immune response	Lorazepam, Temazepam, Alprazolam (12)
GLUL	orf8[2]	Ammonia and glutamate detoxification, acid-base homeostasis	Pegvisomant, L-Glutamine, Methionine (8)
IMPDH1	nsp14[2]	Regulate cell growth	NADH, Ribavirin, Mycophenolate mofetil (7)
S100A13	orf8[2]	Cell cycle progression and differentiation	Calcium (7)
RARA	orf8[2]	Regulation of differentiation of clock genes.	Adapalene, Acitretin, Alitretinoin (7)
MAPK1	nsp13[2]	Differentiation, transcription regulation	Isoprenaline, Arsenic trioxide (6)
SLC16A2	nsp7[2]	Transporter of thyroid hormone	Pyruvic acid, Tyrosine, L-Leucine (6)
CDK4	nsp13[2]	Cell cycle progression	Fostamatinib, Palbociclib, Ribociclib, Abemaciclib
HDAC4	nsp13[2]	Transcriptional regulation, cell cycle progression	Zinc, Romidepsin (4)
PEF1	M[2]	Response to calcium ion	Calcium (3)
CATSPER1	M[2]	Calcium ion transport	Calcium (3)
GNMT	orf8[2]	Methionine metabolic process	Ademetionine, Glycine, Citric acid
PCYT1A	orf8[2]	Regulation of phosphatidylcholine biosynthesis.	Choline, Lamivudine, Choline salicylate
SLC7A1	nsp7[2]	Involved in amino acid transport.	L-Lysine, L-Arginine, Ornithine
YES1	nsp13[2]	Innate immune response; transmembrane receptor protein	Fostamatinib, Dasatinib
ASPH	orf8[2]	Calcium ion transmembrane transport	Aspartic acid, Succinic acid
MAT2A	nsp9[2]	Catalyzes the production of AdoMet	Ademetionine, Methionine
PCNA	nsp15[2]	Positive regulation of DNA repair	Liothyronine, Acetylsalicylic acid
SRR	nsp15[2]	Catalyzes the synthesis of D-serine from L-serine.	Pyridoxal phosphate, Serine
SULT2B1	nsp8[2]	Catalyze sulfate conjugation of many hormones, and drugs.	Prasterone, Pregnenolone

Table 2 | Drugs for the treatment and/or prevention of Covid-19. Fifteen candidate drugs target more than one druggable control hub, among which two belong to immune-related agents (in color), nine are dietary supplements (in green) and two are gonadal hormones (in blue). The drugs with "*" are under clinical trial for the treatment of Covid-19. Detailed information is available in Supplemental Table S5.

Drug	Control hub Number	Control hub
Fostamatinib*	10	COQ8A, CLK3, CLK2, YES1, BLK, PAK5, STK3, RIPK1, PKN1, CDK4
NADH*	5	CYB5R3, EHHADH, HIBADH, NDUFB7, IMPDH1
Calcium phosphate dihydrate	3	S100A13, PEF1, CATSPER1
Calcium Citrate	3	S100A13, PEF1, CATSPER1
Calcium Phosphate	3	S100A13, PEF1, CATSPER1
Conjugated estrogens*	2	SLC10A1, COMT
Progesterone*	2	SLC10A1, SULT2B1
Phenethyl Isothiocyanate	5	HNRNPF, TPM1,
Ademetionine	3	COMT, GNMT, MAT2A
Copper	2	AHCY, CYB5R3
Aspartic acid	2	ASPH, ACY3
Methionine	2	GLUL, MAT2A
Citric acid	2	HGS, GNMT
Liothyronine	2	PCNA, SLC10A1
Liotrix	2	SLC10A1, SLC16A2

Table 3 | Ten druggable control hubs that are no more than two steps away from the viral S protein. **Protein function**s, **Distance**s to the S protein, and **Drugs** targeting the druggable control hubs are shown. Two of these druggable control hubs, ACE2 and ASGR1, are receptors for SARS-Cov-2's entry. Eight druggable control hubs engage the S protein via another host protein. Detailed information is available in Supplemental Table S7.

Host Protein	**Protein Functions**	**Distance**	**Drugs**
ACE2*	Angiotensin maturation; main receptor for SARS-CoV-2's entry	1	Bromhexine, Hydroxychloroquine, Azithromycin, Hydroxocobalamin, Ascorbic acid, Vitamin D (23)
ASGR1	Cellular response to extracellular stimulus; receptor-mediated endocytosis Receptor for many viruses, probably also act receptor for SARS-CoV-2	1	Von Willebrand factor human
BNIP3	Apoptotic process; defense response to virus	2	Calcium
CALM2	Regulation of calcium ion transmembrane transporter activity	2	Calcium (3)
CALM3	Activation of adenylate cyclase activity; regulation of calcium-mediated signaling	2	Calcium (3)
GPX8	Cellular response to oxidative stress	2	Glutathione
KCNIP3	Regulation of potassium ion transmembrane transport	2	Potassium, Magnesium
KLRC1	Cell surface receptor signaling pathway; innate immune response	2	Infliximab, Adalimumab, Certolizumab pegol (6)
NCALD	Calcium-mediated signaling	2	Calcium
TMPRSS4	Facilitates human coronavirus SARS-CoV-2 infection	2	PMSF

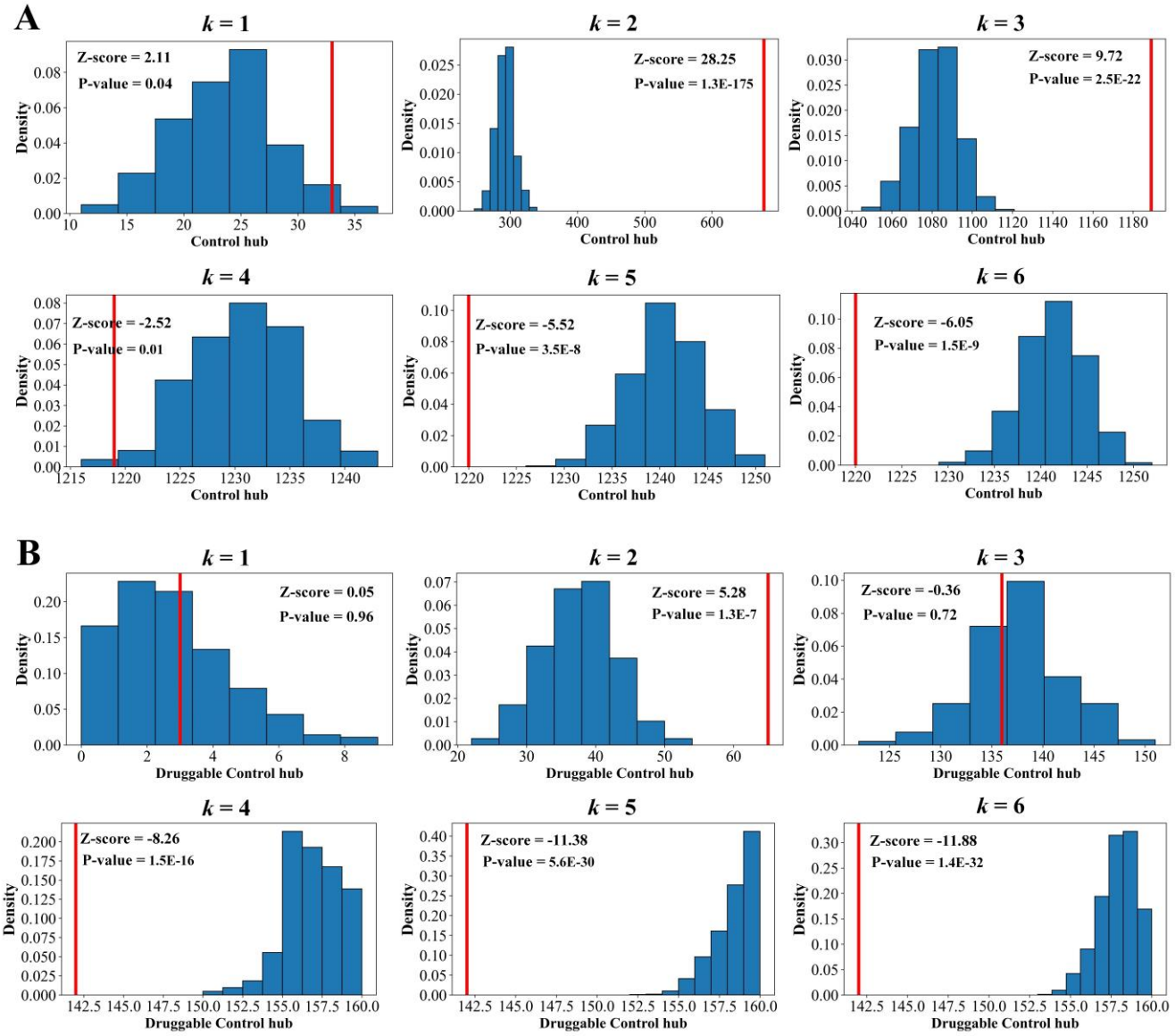

Supplemental Figure S1 | Identification of the community of human proteins *k*-steps away from SARS-CoV-2 proteins which are enriched with control hubs and druggable control hubs. **A)** A series of z-test was adopted to compare the number of control hubs within a *k*-step community against a random empirical distribution (see Methods). The numbers of control hubs within the communities are shown in red lines, and their respective baseline random distributions are shown in blue bars. The 2-step community was enriched with control hubs. **B)** Similarly, the 2-step community was enriched with druggable control hubs.

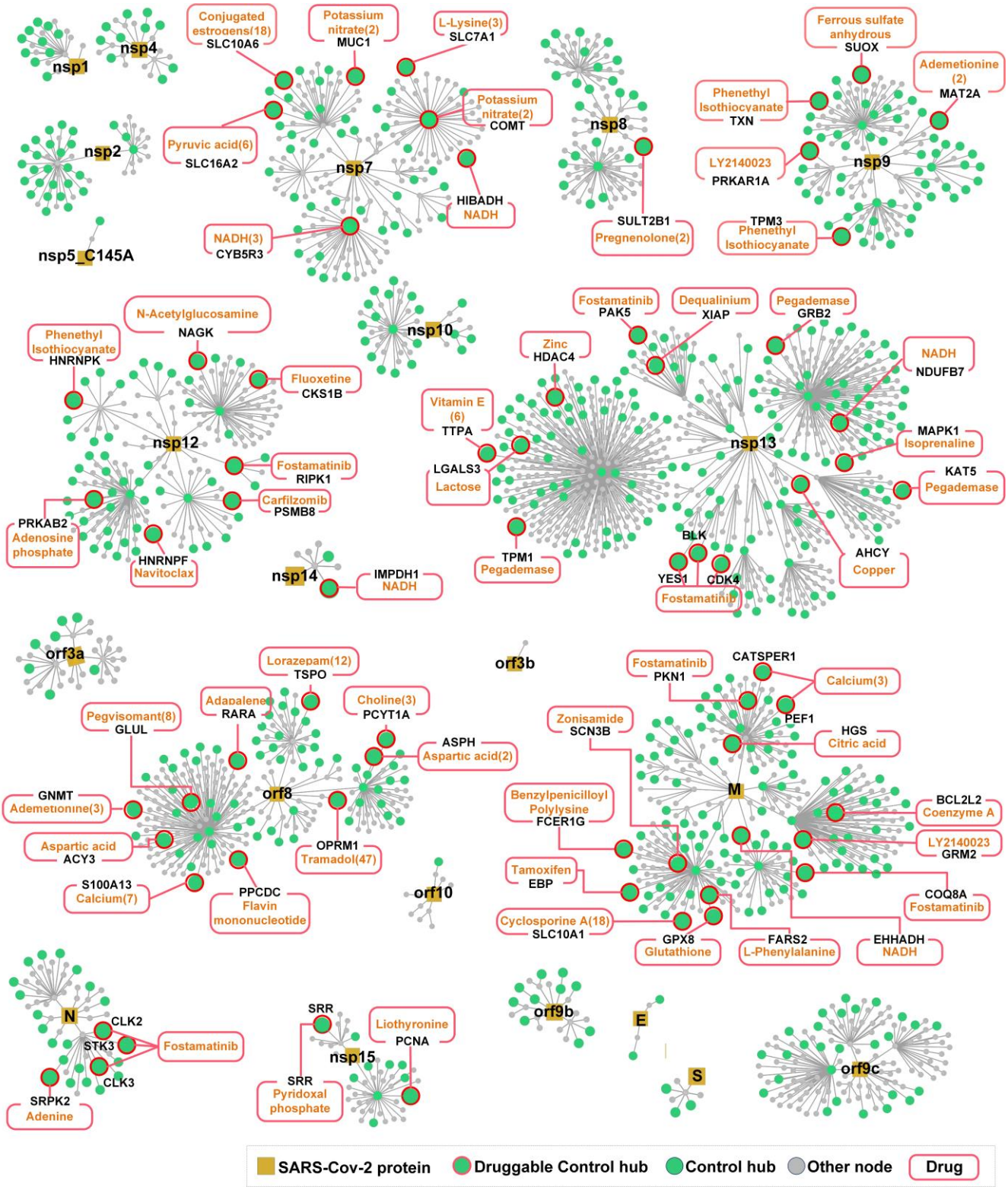

Supplemental Figure S2 | Network topologies of 22 SARS-Cov-2 proteins and 65 druggable control hubs within the 2-step community. The major drugs and the number of drugs targeting the control hubs are shown in red boxes, only one drug is shown for each control hub. The detailed information is available in Supplemental Table S4A.

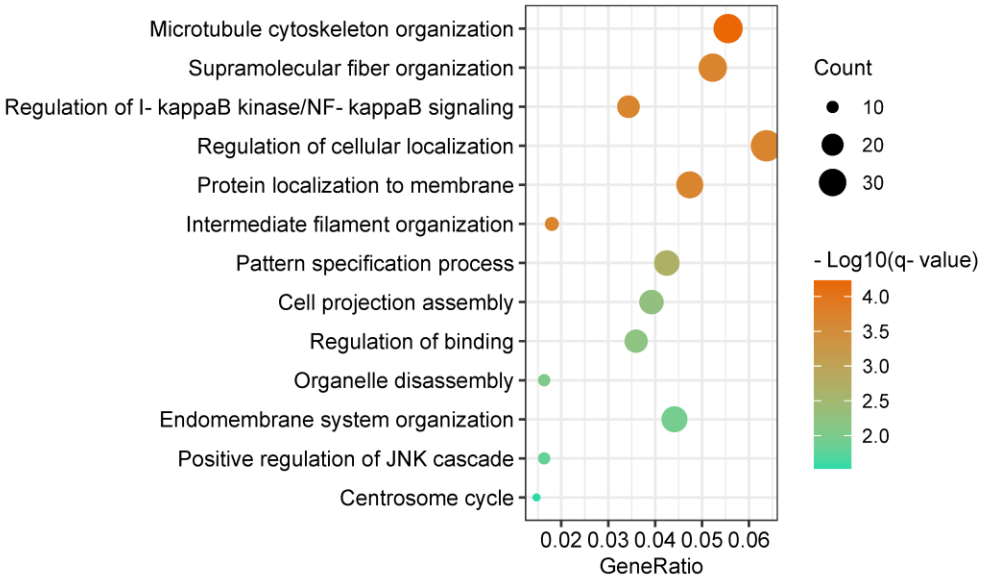

Supplemental Figure S3 | The biological-process enrichment of the 612 non-druggable control hubs within the 2-step community, revealing their collective functions during viral infection. GeneRatio is the ratio between the number of observed proteins and the number of expected proteins with a specific Go term.